Bulletin of the Geological Society of Finland, Vol. 96, 2024, pp 101–134 https://doi.org/10.17741/bgsf/96.2.001

Petrology, geochemistry, and geochronology of the leucogranites in southernmost Finland

Anna Saukko[1*], Kaisa Nikkilä[1], Olav Eklund[1], Sören Fröjdö[1] and Markku Väisänen[2]

[1] *Geology and Mineralogy, Åbo Akademi University, Akatemiankatu 1, 20500 Turku, Finland*
[2] *Department of Geography and Geology, University of Turku, Akatemiankatu 1, 20014 Turku, Finland*

VERTAISARVIOITU
KOLLEGIALT GRANSKAD
PEER-REVIEWED
www.tsv.fi/tunnus

Abstract

In the southernmost part of the Svecofennian province in Finland, leucogranites and migmatites stemming from both igneous and sedimentary protoliths reflect the complex magmatic history of the Svecofennian orogeny between 1.89 and 1.82 Ga. Although the migmatites and leucogranites in southernmost Finland display similar ages as their counterparts elsewhere in the Southern Finland Subprovince, they differ in field appearance and composition. Field and petrographical observations reveal K-feldspar megacrysts of varying sizes in the migmatized early Svecofennian (c. 1.89–1.87 Ga) supracrustal rocks and granitoids. Whole-rock geochemical analyses likewise display anomalously high K-contents in the early Svecofennian granitoids. Zircon U-Pb dating of migmatites and related leucogranites shows that a late Svecofennian partial melting event occurred at 1.84–1.82 Ga, possibly in several pulses. The morphological features of the migmatites as well as neosome mineralogy indicate a formation mechanism different from the dehydration melting prevalent elsewhere in the Subprovince.

Keywords: Svecofennian, Southern Finland Subprovince, migmatite, leucogranite, K-feldspar megacryst, zircon U-Pb, whole-rock geochemistry

*Corresponding author (email: anna.saukko@abo.fi)

Editorial handling: Jarmo Kohonen (email: jarmo.kohonen@helsinki.fi)

1 Introduction

Granitoids are a significant constituent of the Earth's continental crust and understanding the diversity among granitoids is a key to understanding the evolution of the crust. Granitoids are formed in different settings: granitoid magmatism along convergent plate boundaries is a major mechanism for differentiating continental crust from the mantle, whereas partial melting of the crust and subsequent melt ascent to shallow crustal levels is the main process producing granitic (*sensu stricto*) intrusions. In early granitoid classification systems, such as the alphabetic classification scheme created by Chappell & White (1974), different sources were thought to result in specific geochemical compositions, and later classification schemes have aimed to link trace element compositions to tectonic settings (e.g., Pearce 1996). However, geochemically similar granitoids can form from several sources and in different tectonic settings (Frost *et al.* 2001; Bonin *et al.* 2020), making them unreliable indicators of the evolutionary history of an area. Thus, even compositionally simple granites such as leucogranites do not solely form through a single process or from a single source.

Leucogranites are granites characterized by high silica (>70 wt.%) and low mafic mineral (<5 vol.%) contents (Frost *et al.* 2016). They are common in convergent orogens and are thought to mainly form by migmatization, when metapelitic rocks are subjected to dehydration melting of micas, especially muscovite, and the resulting melts escape upwards in the crust to form plutons (Nabelek 2020). However, given the ambiguity in linking any given granitoid to a single source or formation process, leucogranites can also form through other processes. In particular, the role of hydrous fluids in partial melting of the crust has recently gained attention (e.g., García-Arias *et al.* 2015; Weinberg & Hasalová 2015; Schwindinger *et al.* 2019). Influx of water lowers the minimum temperature required for the onset of partial melting and makes a compositionally wide range of metamorphic rocks subject to melting under P-T conditions that in dry systems would not yield melts (Weinberg & Hasalová 2015). Thus, the pressure and temperature path of a migmatite-granite area may be interpreted very differently depending on whether the leucogranite formation process was water-fluxed or not, significantly affecting the P and T evolution estimations for the area.

Leucogranites in southern Finland are a heterogeneous group. Their textures vary from even-grained to porphyritic and grain-sizes from medium to coarse grained. Microcline, quartz, and plagioclase are consistently the major mineral phases in the leucogranites. Of minor and accessory minerals, garnet is common but other mineral phases vary (Kurhila 2011). The leucogranites are part of the late Svecofennian granite magmatism, their ages spanning from around 1850 to 1790 Ma, (Kurhila *et al.* 2005; Nironen & Kurhila 2008). They have typically crystallized among or close to migmatites so the transition from migmatites to granites is gradual rather than sharp (Kurhila *et al.* 2005). Some leucogranite intrusions have been interpreted as having intruded along subhorizontal shear zones (Ehlers *et al.* 1993).

Like most leucogranites, the Svecofennian leucogranites are thought to have formed when metasupracrustal protoliths were subjected to "dry" (dehydration) melting, where no external fluids were required to initiate the melting reactions (Mengel *et al.* 2001; Johannes *et al.* 2003; Andersen & Rämö 2021). The commonly suggested peak metamorphic conditions at the time of the leucogranite formation in the Southern Svecofennian Subprovince are 700–800 °C and 3–6 kbar. The protoliths are mixtures of older metaigneous and metasedimentary rocks: the metaigneous rocks are generally the most significant source material (Andersen & Rämö 2021), but metasedimentary protoliths are important in the western and eastern parts of the Subprovince (Mengel *et al.* 2001; Johannes *et al.* 2003; Kurhila *et al.* 2005; Mäkitie *et al.* 2019). The host rocks that surround the leucogranites display the same diversity, being mainly metavolcanic and metagranodioritic in the central part of the

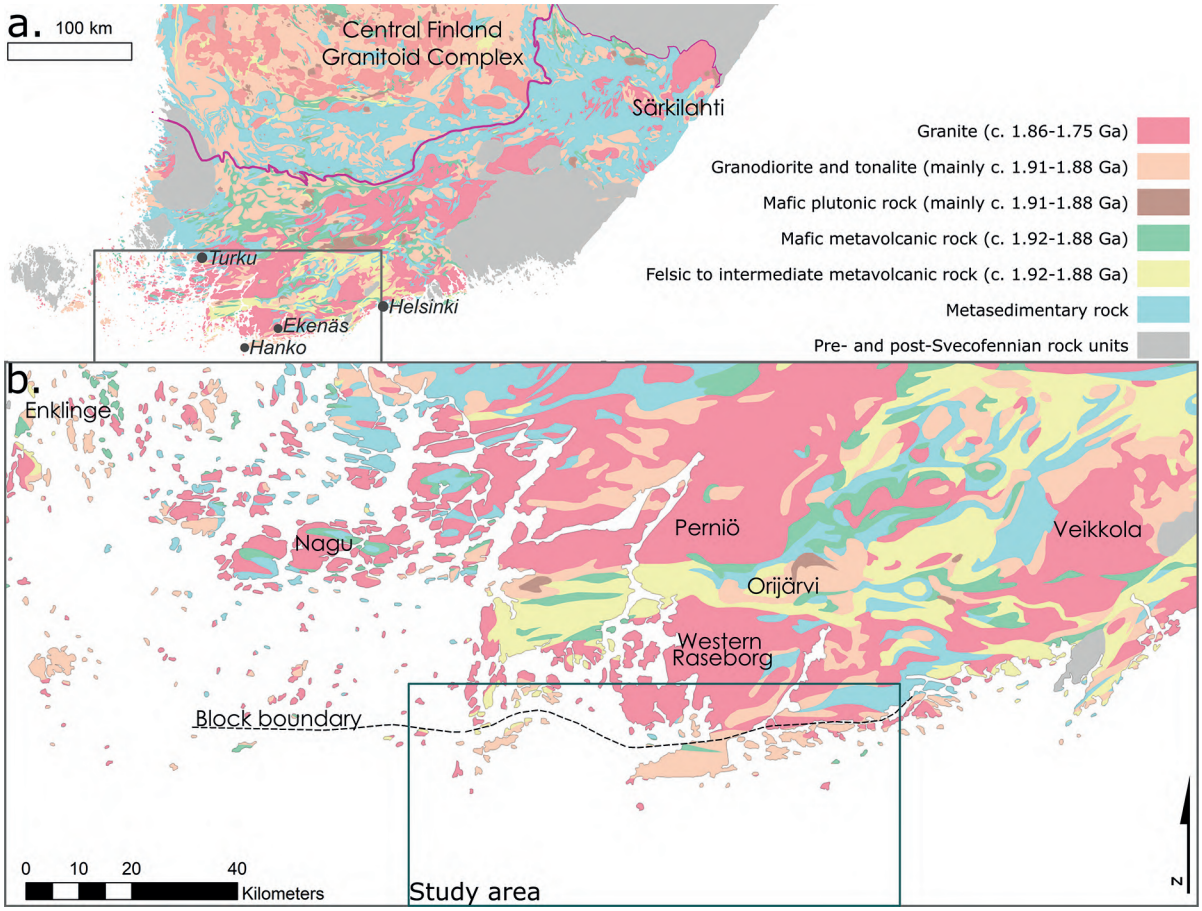

Fig. 1. a) Lithological map of the Southern Svecofennian Subprovince with its borders marked by the magenta line (Geological Survey of Finland 2001). b) Close-up of the lithological map. The block boundary is drawn according to Edelman & Jaanus-Järkkälä (1983). The named locations outside of the study area denote previously researched areas referred to throughout the paper.

Subprovince, and metapelitic in the western and eastern parts (Fig. 1a).

The leucogranite in our study area in the Hanko-Ekenäs area, first described by Sederholm (1907) (called the Hangö or Hanko granite), has some key differences compared to other granites in the late Svecofennian leucogranite group. Firstly, the granite contains little garnet and, instead, contains opaque minerals that are uncommon in the other leucogranites (Kurhila *et al.* 2005). Secondly, most late Svecofennian leucogranites yield similar monazite and zircon ages (Kurhila *et al.* 2005), recording the same crystallization event, but previous zircon analyses from the leucogranite in Hanko have shown heavily altered zircon with imprecise but apparently older U-Pb ages than monazites (Huhma 1986; Suominen 1991; Kurhila *et al.* 2005). Given that Edelman & Jaanus-Järkkälä (1983) have proposed that the area is separated from the rest of the subprovince by a subduction-related mélange zone, the differences in leucogranites may result from the southernmost Finland leucogranite originating from different protoliths and processes than the other late Svecofennian leucogranites, and perhaps being at a different exposure level.

To examine the leucogranites and associated migmatites of southernmost Finland, we describe the mineralogical, petrographical, and whole rock

geochemical features of the different rock types of the area south of the Hitis shear zone in Hanko and Ekenäs. To better constrain the ages of the rock types and the late Svecofennian partial melting event, we publish new zircon U-Pb data. We show that leucogranites in southernmost Finland stem from water-fluxed melting of earlier granitoids and heavily altered supracrustal units.

2 Geological setting

2.1 Regional geology

The Paleoproterozoic Svecofennian orogen is thought to have formed through a complex and semi-continuous set of orogenic events between 1920 and 1770 Ma (Lahtinen *et al.* 2005; Korja *et al.* 2006; Nironen *et al.* 2017). During the long Svecofennian orogeny, the pre-existing Karelian craton experienced a phase of continental growth, either through an accretionary orogeny followed by a continental collision (Lahtinen *et al.* 2009; Nironen *et al.* 2017), or through a single long-lived accretionary orogeny in a subduction system (Hermansson *et al.* 2008; Stephens & Andersson 2015; Stephens 2020). The Paleoproterozoic domain of the continent is known as the Svecofennian Province, and its Finnish part consists of two lithotectonic units: the Western and Southern Finland Subprovinces (Luukas *et al.* 2017). The Western Finland Subprovince consists of magmatic arc granitoids (Elliott 2003; Nikkilä *et al.* 2016) surrounded by metasedimentary and metavolcanic schist belts that have, in some cases, undergone significant anatexis and accommodated the anatectic melts as granitoid intrusions (Suikkanen *et al.* 2014; Chopin *et al.* 2020). The Southern Finland Subprovince, on the other hand, contains volcanic belts interspersed with zones of mainly sedimentary rocks that have been strongly migmatized and partly intruded by leucogranites (e.g., Ehlers *et al.* 1993).

The Southern Finland Subprovince consists of originally volcanic, sedimentary, and plutonic rocks (Ehlers *et al.* 1993; Kähkönen 2005) that underwent middle amphibolite to granulite facies metamorphism during the Svecofennian orogeny (Hölttä & Heilimo 2017). The timing and characteristics of early volcanism in the Southern Finland Subprovince are well constrained due to studies of the two E-trending volcano-sedimentary belts in the area, the Häme and Uusimaa belts. Radiometric dating of zircon has shown that the volcanic belts were formed at approximately 1900–1880 Ma (Patchett & Kouvo 1986; Väisänen & Mänttäri 2002; Kähkönen 2005). The Häme belt to the north is compositionally the more juvenile of the two (Lahtinen 1996; Kähkönen 2005). The sedimentary rocks were, in part, deposited concurrently with the volcanic rocks (Kähkönen 2005), and in part after the main accretionary phase (Nironen 2011).

The oldest granitoids of the Southern Finland Subprovince are mainly intrusive tonalite, trondhjemite and granodiorite (TTG) like rocks that crystallized at 1890–1870 Ma (Väisänen & Mänttäri 2002; Saalmann *et al.* 2009; Väisänen *et al.* 2012a). Hopgood *et al.* (1983) and Ehlers *et al.* (1993) proposed that a partial melting episode occurred in southern Finland at this time, and Skyttä (2007) further thought that this early migmatization occurred in the lower levels of the crust. A magmatic event associated with extensional tectonics occurred at around 1865–1840 Ma (Väisänen *et al.* 2012a; Kara *et al.* 2020). This magmatism included both mantle- and crust-derived components and resulted in both mafic and felsic intrusive rocks (Väisänen *et al.* 2012a; Nevalainen *et al.* 2014).

A later metamorphic culmination and related migmatization in the Southern Finland Subprovince took place at around 1830–1820 Ma in high amphibolite to low granulite facies (Väisänen & Hölttä 1999; e.g., Mouri *et al.* 2005). In the south, partial melting was extensive, and leucogranites related to the migmatization are very common (Ehlers *et al.* 1993; Johannes *et al.* 2003). Leucogranite crystallization occurred during a long time period from 1850 to 1790 Ma, with the leucogranites to the east being slightly younger than

their western counterparts (Kurhila 2011). Due to the spatial association with metasedimentary migmatites and because of their major element compositions, the Svecofennian leucogranites were originally thought to be mainly derived from metasedimentary sources (e.g., Nurmi & Haapala 1986). Later isotope studies have shown that the sources were more diverse, comprising both metaigneous and metasedimentary components (Kurhila *et al.* 2010). As the leucogranites are peraluminous and very little mafic magmatism is associated with them (Kurhila 2011), their sources are likely crustal (Patiño Douce 1999). Crustal melts are commonly thought to be transported along shear zones (e.g., Brown 1994), and this is the case also in the Southern Finland Subprovince where shear zones have been interpreted as pathways for the magmatism in the area (Selonen *et al.* 1996; Stålfors & Ehlers 2006).

2.2 Study area

The study area covers an approximately 30 by 80 km large area in the southernmost archipelago of Southern Finland. Bedrock maps (Edelman 1954; Laitala 1970, 1973; Nironen *et al.* 2016; Fig. 2a) classify the outer archipelago to the south as migmatitic granite. The inner archipelago and mainland are more heterogeneous, comprising E-trending belts of a wide variety of originally supracrustal and plutonic metamorphic rocks appearing as alternating bands (Fig. 3a). Edelman (1954) classified the heterogenous, quartz- and plagioclase-bearing rocks with amphibolite and marble interlayers predominantly as acid banded series and quartz-feldspar gneiss, whereas Laitala (1970, 1973) classified it as granodiorite. We use the name quartz-feldspar paragneiss, as it is the currently used name based on Edelman's classification (Geological Survey of Finland 2014) and best corresponds to our field observations (Fig. 2b). Based on field observations of partial melting and deformation in a megacryst-bearing granitoid, we call the microcline granite in the southern part of the study area (Fig. 2a) a granitic metatexite.

Foliation in the study area is predominantly E-trending and steeply dipping (Laitala 1970, 1973), and NE-SW oriented shear zones, like the Barösund shear zone (Fig. 2; BSZ), deflect the foliation (Laitala 1970, 1973). The other shear zones in the area are the WNW-striking Southern Finland shear zone (SFSZ) in the west (Nordbäck *et al.* 2023), the E-striking Hitis shear zone in the north (Edelman & Jaanus-Järkkälä, 1983; Nordbäck *et al.* 2023).

The granites and migmatites of the area were first described by Sederholm (1907), who noted the visual similarity between granitic leucosomes and leucogranites in the area, and therefore suggested that the leucogranites had originated from the migmatites. Later, Sederholm (1926) proposed that fluids associated with granite plutons may cause mineral alteration in the host rocks, rendering the composition of the host rocks more granite-like.

Previous zircon U-Pb dating shows that strongly metamorphic mafic rocks from the study area are of ages between about 1900 and 1880 Ma (Hopgood *et al.* 1983), corresponding to the volcanism dated in the Häme and Uusimaa belts. Similar ages, around 1895 Ma, have been obtained from zircon from leucosomes in an amphibolitic migmatite (Bredenberg 2019), indicating that either the partial melts or the protoliths were formed during this stage. U-Pb dating of rocks associated with a crustal-scale shear zone to the northeast of our study area has revealed an 1889 ± 10 Ma old porphyritic granite, and an 1877 ± 11 Ma old tonalite (Vehkamäki 2019) corresponding well with the TTG-like magmatism ages reported elsewhere in the Southern Finland Subprovince (Väisänen *et al.* 2012b; Kara *et al.* 2018).

Dating of younger Svecofennian rocks in the area has mainly targeted the loosely defined Hanko granite, an even-grained leucogranite that contains nebulitic remains of an older rock (Huhma 1986; Kurhila *et al.* 2005). Monazite ages of the granite are around 1830–1820 Ma (Huhma 1986; Suominen 1991), whereas zircon ages are slightly older and less precise at 1852 ± 18 Ma (Kurhila *et al.* 2005).

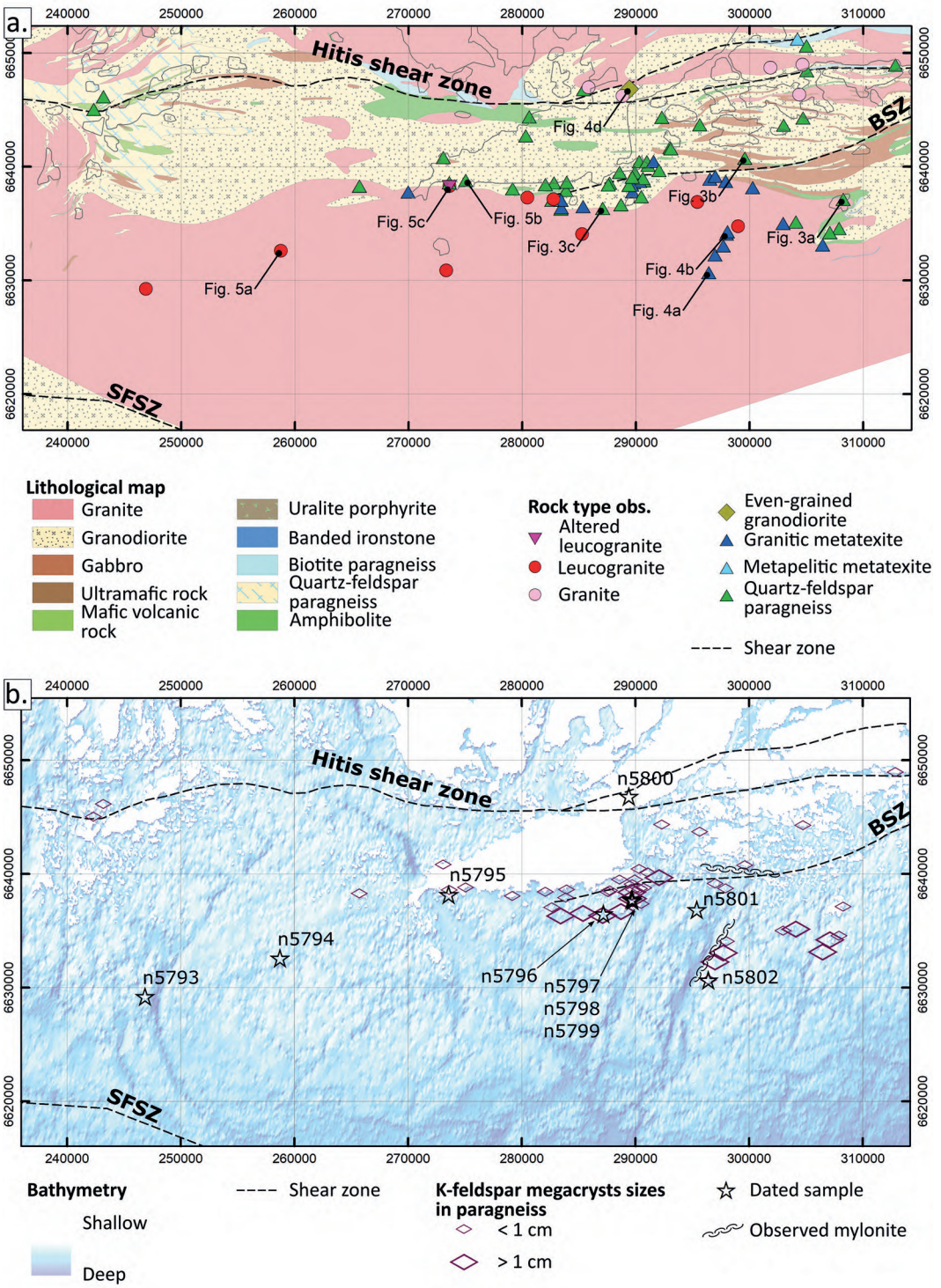

Fig. 2. a) Pre-existing lithological map (Geological Survey of Finland 2014) of the study area with previously described shear zones (Edelman & Jaanus-Järkkälä 1983; Geological Survey of Finland 2001; Nordbäck *et al.* 2023). Major rock type observations are those made in this work. b.) Bathymetric map (EMODnet Bathymetry Consortium 2018) of the study area with the locations of dated samples, observed mylonites and K-feldspar megacryst sizes in quartz-feldspar paragneiss. SFSZ – Southern Finland shear zone, BSZ – Barösund shear zone.

3 Sampling and analytical methods

3.1 Sampling, nomenclature, and mapping

For this work, we collected altogether 45 rock samples of seven different rock types in the study area: quartz-feldspar paragneisses (n = 7), granitic metatexites (n = 10), leucocratic dikes, veins or leucosomes (n = 7), grey leucogranites (n = 8), red leucogranites (n = 5), an altered leucogranite (n = 1), and even-grained granodiorites (n = 7). Many sampling and observation sites are on small islets and skerries.

Following the migmatite nomenclature by Sawyer (2008), we refer to all light-colored neosomes consisting mainly of quartz and feldspars with the general term leucosome, and use the same nomenclature in subdividing them into *in situ* and in-source leucosomes, and leucocratic veins and dikes, based on their petrogenetic relationships with their hosts. The leucosome samples we discuss here are in-source leucosomes and leucocratic dikes, containing the light-colored parts formed through crystallization of partial melt, but no melanosome. In contrast, metatexite, as defined by Sawyer (2008), is a migmatite that is a heterogeneous rock where features predating the partial melting are preserved in the paleosome and, possibly, residuum. Our quartz-feldspar paragneiss and granitic metatexite samples represent the bulk migmatite focusing on the paleosome but not excluding residuum or *in situ* leucosomes. The petrographical features of each rock type are summarized in Table 1.

3.2 Zircon U-Pb dating

To define the temporal variation in the rock types, we chose 10 samples for zircon U-Pb analyses. We hand-picked the zircons after heavy liquid and magnetic separation of crushed samples, then mounted them on epoxy. After polishing and gold-coating, the mounts were imaged in BSE (back scatter electron) with a JEOL IT-100 InTouchScope Scanning Electron Microscope at Top Analytica Oy Ab to study the internal structures of the zircons and to locate suitable spots for beam analysis. The zircons were analyzed with a CAMECA IMS1280 large-geometry ion microprobe at the NordSIMS facility in Stockholm, closely following the procedures described by Whitehouse & Kamber (2005). An O_2 primary beam of ca. 6 nA and 23 kV impact energy was used, producing an aperture illuminated spot of approximately 15 μm (slightly elliptical long axis). The mass resolution (M/DM) was 5400. Isotope signals were measured in a low noise ion counting electron multiplier. The raw data Pb/U ratios were calibrated against Geostandards zircon 91500, which has an age of 1062.4 Ma (Wiedenbeck et al. 1995), following the protocols of Jeon & Whitehouse (2015). Electronic Appendix A contains the compiled analytical data.

3.3 Major and trace element analyses

Whole-rock geochemical analyses on leucogranite and migmatite samples (MIGMA-samples) were done in part at commercial laboratories and in part at the university laboratories at the Geohouse, Turku. 16 whole-rock samples were analyzed at the Activation Laboratories (Actlabs) in Canada, seven samples (MJV-samples) at Acme Analytical Laboratories Ltd. (Acme) in Vancouver, Canada, and 20 samples in the Geohouse laboratories. The used analytical methods are described in Electronic Appendix B.

We processed the geochemical data using the GCDKit software (Janoušek *et al.* 2006). We acknowledge the uncertainty stemming from the inherent heterogeneity in outcrop and sample scale, and also from using analytical data obtained through different methods and laboratories. To accommodate this, we focus on general trends instead of exact element contents in our analysis and avoid elements that display large discrepancies between the different laboratories. In the

Table 1. Mineral composition, textures, and alterations of the studied rock types

Rock type	*Representative sample*	*Mineral composition*	*Accessory minerals*	*Textures*	*Alteration*
Megacryst-bearing quartz-feldspar paragneiss	n5797 Figure 2 B and C	**Plagioclase, quartz, orthoclase, microcline, biotite** ± hornblende	zircon, muscovite, apatite	Orthoclase megacrysts varying in size from 5 to 30 mm, matrix 1–3 mm Myrmekite	Sericitization, microclinitization of orthoclase. Biotite breakdown into opaque crystals (<0.05 mm across) and quartz
Granitic metatexite	n5798 n5802 Figure 2 B and D	**Plagioclase, quartz, orthoclase, microcline, biotite** ± titanite	zircon, muscovite, apatite, ilmenite	Orthoclase megacrysts varying in size from 5 to 50 mm, matrix 2–5 mm Abundant myrmekite	Sericitization, microclinitization of orthoclase. Biotite breakdown into an opaque phase, quartz, monazite, and titanite
Leucosome and leucocratic vein	n5796 n5799	**Quartz, plagioclase, orthoclase, microcline,** biotite	muscovite, zircon, apatite	Even-grained, grain size 1–5 mm Some myrmekite	Sericitization, microclinitization of orthoclase. Biotite breakdown
Even-grained granodiorite	n5800	**Plagioclase, quartz, orthoclase, biotite** ± hornblende, microcline	apatite, muscovite, zircon, chlorite,	Even-grained, grain size 1–5 mm Abundant myrmekite	Sericitization, saussurization, microclinitization of orthoclase. Biotite breakdown
Grey leucogranite	n5793 n5794	**Quartz, plagioclase, microcline, orthoclase,** biotite	muscovite, zircon, apatite, chlorite, magnetite	Mainly 0.5–3 mm, some up to 10 mm orthoclase phenocrysts Quartz with undulose extinction	Strong sericitization, microclinitization of orthoclase. Biotite breakdown
Red leucogranite	n5801 Part of n5795	**Quartz, plagioclase, orthoclase, microcline,** biotite ± garnet	chlorite, muscovite, apatite	Even-grained, grain size 1–5 mm Some myrmekite	Sericitization, microclinitization of orthoclase. Biotite breakdown Cracks with red filling (Hanko sample)
Altered leucogranite	Part of n5795	**Orthoclase, plagioclase, microcline,** biotite, quartz	monazite, muscovite, epidote, apatite, chlorite, zircon	Even-grained, 2–6 mm Some myrmekite	Sericitization, microclinitization of orthoclase. Biotite breakdown cm-scale microclinitized feldspar with mineral inclusions (cf. quartz and biotite)

supplementary data, we also include a comparison of the results for the subset of samples that were analyzed at two different laboratories. The results are reported in Table 2 (major elements only) and Electronic Appendix B (full data set).

4 Field relations and petrography

4.1 Migmatites

Both volcano-sedimentary and plutonic rocks in the area have undergone partial melting and now appear as metatexitic migmatites, which we call quartz-felspar paragneisses and granitic metatexites, respectively. The quartz-feldspar paragneisses occur in many places of the study area, whereas granitic metatexites nearly are absent at the mainland and mainly visible on the islets and skerries to the south (Fig. 2). The most notable features of the migmatites are the orthoclase megacrysts that are present not only in the granitic metatexites, but also in many quartz-feldspar paragneisses (Fig. 3b, c). Although the megacrysts appear as single grains with the naked eye, polarization microscopy reveals that they consist of many smaller grains surrounding a larger central grain.

Due to similar mineral compositions, the conspicuous orthoclase megacrysts, and heavy deformation, distinguishing between plutonic and supracrustal rocks is difficult at some places. However, the granitic metatexites have homogenous and even-grained matrices, whereas the matrix grain size of the paragneisses varies and they contain deformed, layer-like structures.

4.1.1 Quartz-feldspar paragneisses

The protoliths to the quartz-feldspar paragneisses in the area were extrusive volcanic rocks together with volcaniclastic and other sedimentary rocks (Hopgood *et al.* 1976). In the northern part of the study area, primary properties are better preserved than further south. To the south, the quartz-feldspar paragneisses contain more neosome, and most of them also contain orthoclase megacrysts that vary in size between different outcrops. We found relatively small, 0.5–1 cm sized, secondary orthoclase megacrysts in intermediate volcanogenic layers to the north of the study area, but larger megacrysts generally occur further to the south and closer to the major shear zones. On the outcrop scale, the more mafic rock units contain smaller megacrysts than the more felsic units (Fig. 3b). The abundant megacrysts make some of the quartz-feldspar paragneisses in the south appear very similar to the granitic metatexites, but field observations suggest that the protolith to the granitic metatexites intruded into the quartz-feldspar paragneisses (Fig. 3c; Sederholm 1907; Edelman 1960; Edelman & Jaanus-Järkkälä 1983).

The large orthoclase megacrysts in quartz-feldspar paragneisses display no magmatic zoning. They contain small (around 100 µm long and smaller) inclusions of biotite and zircon, which are mostly parallel with and perpendicular to the foliation. Biotite also occurs as clusters of a few grains, or as long and narrow bands in the matrix. Most of the accessory phases, such as zircon and monazite, are situated among biotite (Fig. 3d). Two different types of biotite occur in the migmatites: some have well-formed crystal structures, whereas others are heavily altered and have partly turned into very fine-grained ilmenite.

The megacryst-free quartz-feldspar paragneisses are a heterogeneous group, varying in mineral compositions due to protolith differences. Different felsic volcanic rocks, amphibolites and metapsammitic rocks are the most common protoliths to quartz-feldspar paragneisses, but some interlayers of carbonate rocks and metapelite occur among them. Quartz-feldspar paragneiss grain sizes vary, but all display evidence of metamorphic coarsening. Some quartz-feldspar paragneiss layers consist of flecked gneiss featuring magnetite and hornblende flecks surrounded by light-colored haloes of quartz, orthoclase, and sericitized plagioclase. The shapes of the haloes range from nearly round in some layers to elongated and connected in others.

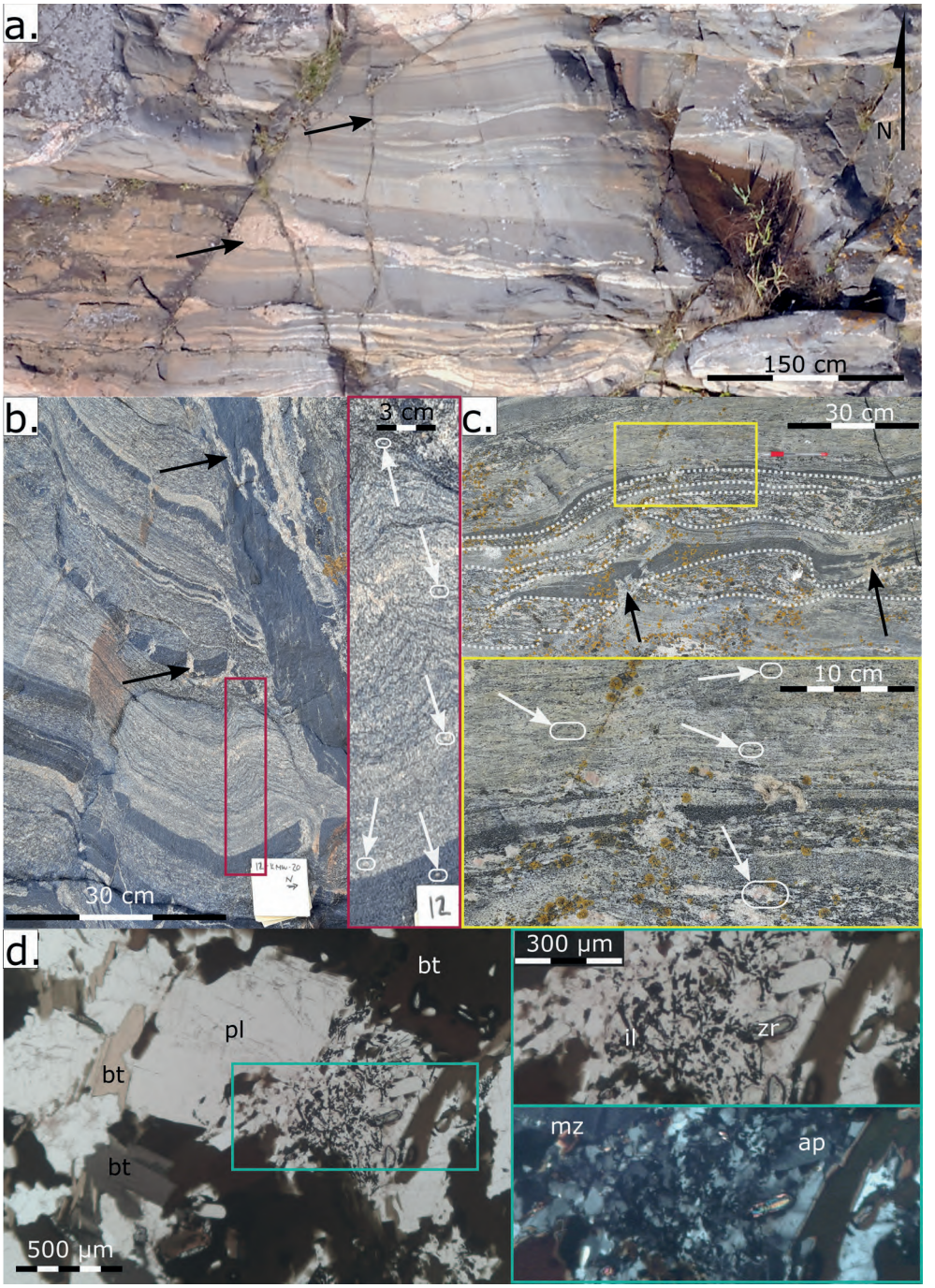

Fig. 3. Field and microscope pictures of paragneisses where K-feldspar megacrysts are marked with white and leucosomes with black arrows. a) Drone image of migmatized supracrustal rocks. The darkest bands are mafic and the grey bands intermediate to felsic volcanogenic units. b) Migmatized supracrustal rocks likely reflecting primary bedding with small K-feldspar megacrysts present in different layers. Leucosomes appear as both dilational and parallel to the compositional layering. c) Granitic metatexite (marked by dashed lines) in quartz-feldspar paragneiss. Both rock types contain cm-scale K-feldspar megacrysts. d) Photomicrographs of a quartz-felspar paragneiss displaying accessory minerals located among biotite grains. The bottom right image is cross-polarized, the others plane polarized. Abbreviations: pl=plagioclase, bt=biotite, il=ilmenite, zr=zircon, mz=monazite, ap=apatite.

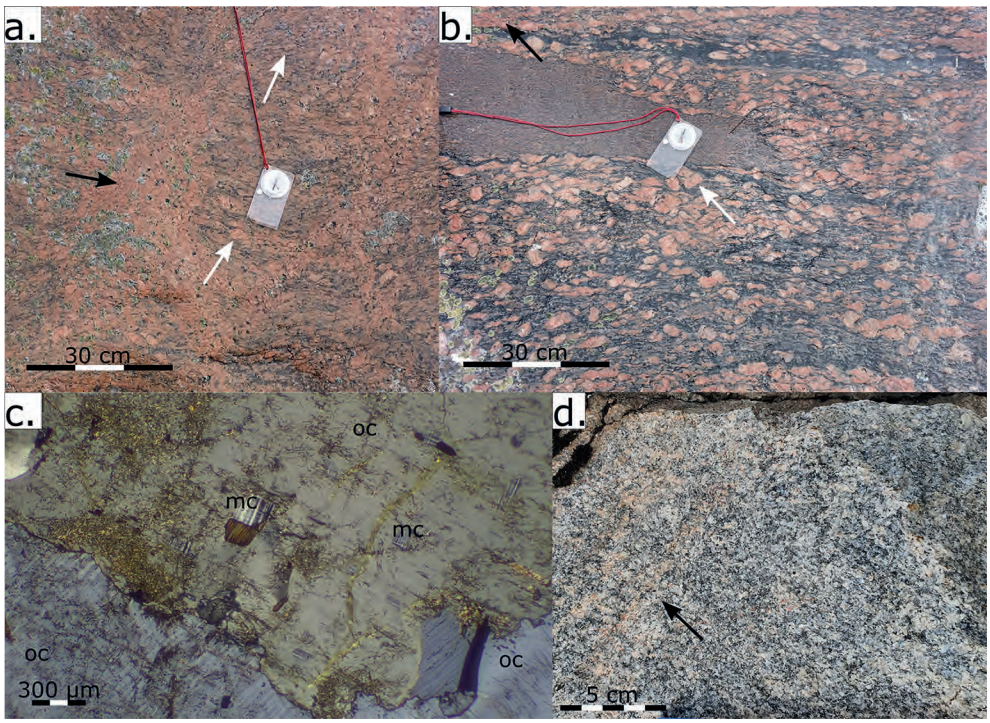

Fig. 4. Field and microscope pictures of old granitoids. K-feldspar megacrysts are marked with white and leucosomes with black arrows. a) Leucosome in granitic metatexite. K-feldspar megacrysts are prominent. The black minerals in the leucosome are peritectic hornblende. b) Mylonitic granitic metatexite with a supracrustal raft. c) Cross-polarized photomicrograph of a orthoclase with microcline patches in a granitic metatexite. Abbreviations: oc=orthoclase, mc=microcline. d) Even-grained granodiorite. K-feldspar rich, light-colored veins and patches with diffuse contacts occur in the granodiorite.

4.1.2 Granitic metatexites

Metatexites formed through partial melting of granitoid protoliths are generally parallel to the quartz-feldspar paragneisses (Fig. 3c), but some crosscutting occurs in lithological contacts, suggesting that the granitoid formed sheet-like intrusions in supracrustal layers. The granitic metatexites are more homogeneous than the megacryst-bearing quartz-feldspar paragneisses, and unlike them, do not display any compositional changes corresponding to original supracrustal layering (Fig. 4a). They are mainly mylonitic and found in proximity to shear zones (Fig. 4b, Fig. 2). Mineralogically, the granitic metatexites are similar to the megacryst-bearing quartz-feldspar paragneisses. Orthoclase megacrysts in the granitic metatexites contain microcline inclusions (Fig. 4c) and display weak zoning. Biotite and zircon inclusions in the megacrysts are fewer than in the paragneisses and display no preferred orientation.

4.1.3 In-source leucosomes and leucocratic dikes

Unambiguous *in situ* leucosomes are uncommon in the study area, because deformation during partial melting caused melt movement. Instead, in-source leucosomes are common, appearing as mm-to-cm-scale veins either parallel, oblique, or perpendicular to the compositional layering (Fig. 3b). In our study area, they have gradual, diffuse, and sinuous contacts to the hosts. In appearance, they are distinct from the younger granite and pegmatite dikes, which crosscut the migmatites with sharp contacts, and which are not considered here as they were not formed from local melts.

Most leucosomes are red in color and contain significant amounts of K-feldspar, but leucosomes in proximity with mafic paleosomes are whiter in color. Contacts between leucosomes of different colors are rare, but the few contacts we found show red leucosomes crosscutting the white, indicating that they crystallized later. Biotites in the leucosomes display crystal habits similar to those in the metatexites – some grains are euhedral, whereas others have altered into secondary minerals – but are present in smaller quantities.

Melanosomes are mostly absent but where present, they usually occur as peritectic Fe-rich hornblende at the diffuse borders or in the centers of leucosomes (4a). Mica-rich melanosomes lining leucosomes as distinct stripes are rare, occurring only in the volumetrically minor, metapelitic units. The diffuse, gradual borders between leucosomes and their hosts complicate the classification of migmatite parts, because some metatexite matrices and leucosomes are very similar in mineral composition. Most leucosomes have been folded or bent under stress. Leucosomes do not have schistosity, but they often follow the E-trending foliation of the host rocks.

4.2 Even-grained granodiorites

The even-grained granodiorites (Fig. 4d) have a weak foliation and occur mostly in the Hanko peninsula, close to the Hitis shear zone. They range in composition from orthoclase-poor and hornblende-rich *sensu stricto* granodiorites to orthoclase-rich, granitic variants. In contrast to the leucogranites, they contain substantially more of mafic minerals, and plagioclase is more abundant than K-feldspar. The grain sizes are around 1–4 mm, and major minerals are quartz, plagioclase, and in some samples also orthoclase. Biotite is the most common mafic mineral, but hornblende is also abundant in some samples. The granodiorites that contain more orthoclase host granitic portions in the form of pink stripes that have gradual contacts to the granodiorite. The grain size and orientation of the granodiorite are unchanged in the granitic stripes, but the stripes contain more K-feldspar than the host. This indicates that the granodiorites were either partially melted or altered by fluids.

4.3 Leucogranites

The leucogranites are even-grained granites, which generally have grain sizes 1–5 mm and contain little dark minerals, much less than the observed granites to the north of the Hitis shear zone (Fig. 2a). They mostly occur in the middle of study area, south of the Hanko peninsula (Fig. 2). We further classify the leucogranites into red and grey leucogranites based on their color but emphasize that this classification is a spectrum rather than binary: some leucogranites are somewhere in between of the two endmembers. Most leucogranites contain some metatexite rafts (Fig. 5a, b), and in some outcrops metatexites are present next to tens of meters wide leucogranites, implying that the observable leucogranites have not wholly escaped the anatectic system they were formed in and might be considered diatexites instead of granite intrusions.

4.3.1 Grey leucogranites

The grey leucogranites (Fig. 5a) mainly occur in the western part of the study area (Fig. 2). On the westernmost outcrops, the granite is massive and contains little paleosome, but closer to the Hanko peninsula, more paleosome is present. The grey leucogranites contain magnetite flecks with light-colored haloes around them, reminiscent of the flecked gneiss layers in some quartz-feldspar paragneisses. On Bengtskär island (n5793; Fig. 1), the magnetite flecks are around 5 mm in size and the light halos around them up to 10 mm wide. On Morgonlandet (n5794; Fig. 1), the dark flecks are up to 3 cm in size, consisting of clusters of multiple grains. The haloes are also larger, up to 5 cm wide, and in some places multiple haloes are connected as longer stripes with dark flecks inside them.

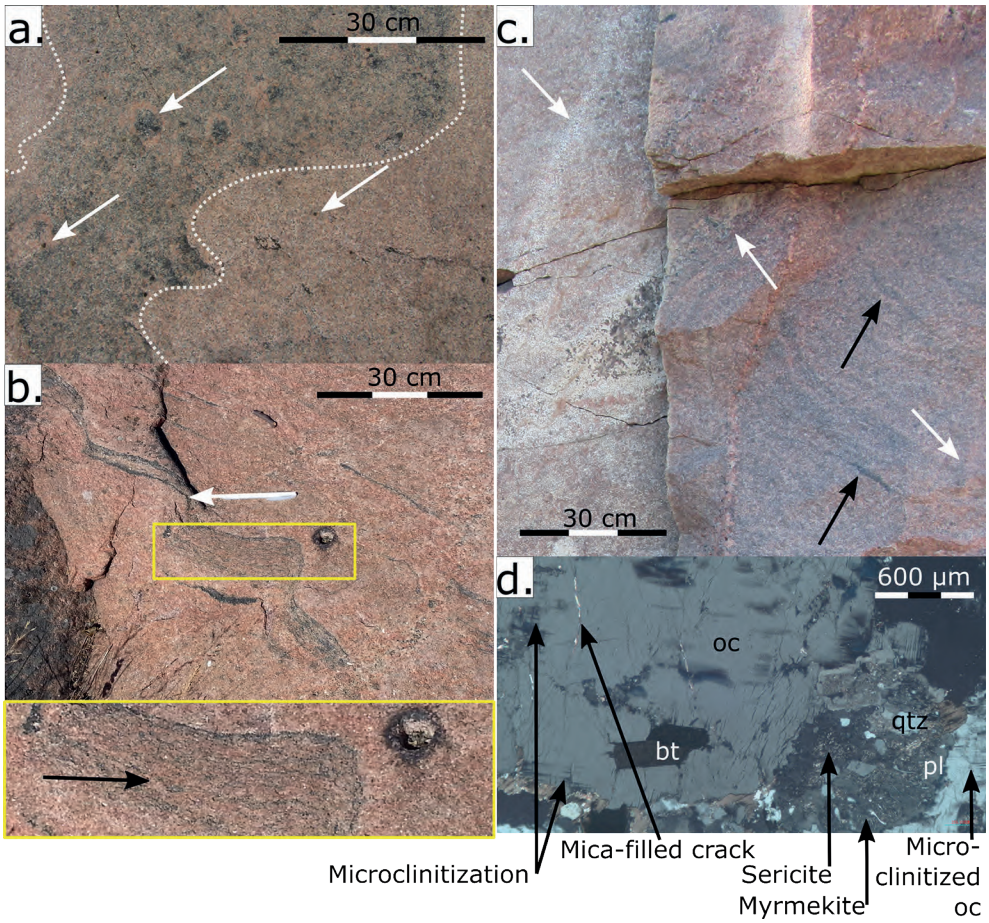

Fig. 5. Field and microscope pictures of the leucogranites. a) Paleosome raft (between the dashed lines) in grey leucogranite. The paleosome contains cm-scale aggregations of magnetite and amphibole surrounded by distinctive light-colored haloes, whereas in the leucogranite the dark minerals appear as single grains and with less distinctive haloes (arrows). b) The red leucogranite contains plenty of largely assimilated remains of its protoliths (white arrow). Deformed K-feldspar megacrysts (black arrow) are visible in the least assimilated paleosome raft. c) Kuningattarenvuori altered leucogranite outcrop. The alteration appears as light-colored veins with diffuse boundaries (white arrow) criss-crossing the granite. The granite also contains some paleosome schlieren (black arrows). The U-Pb dating was done on a sample containing both altered and unaltered portions whereas the geochemical analysis was done on the altered portions only. d) Cross-polarized photomicrograph of the altered leucogranite in c. Many minerals are altered, and quartz is only present in minor amounts. Abbreviations: pl=plagioclase, bt=biotite, qtz=quartz, oc=orthoclase.

4.3.2 Red leucogranites

Red leucogranites (Fig. 5b) mainly outcrop on islands to the south of Hanko peninsula. Microclinization is visible in orthoclase, but microcline does not appear as separate crystals. Biotite contains monazite inclusions, but the red leucogranites contain very little zircon. Heavily altered garnet is present in some of the red leucogranites, but not in any other major rock types in the study area. Compared to the grey leucogranites, the red leucogranites contain even less mafic minerals.

4.3.3 Kuningattarenvuori altered leucogranite

At one location, on Kuningattarenvuori (n5795, Fig. 1), the red leucogranite contains quartz-poor portions appearing as veins that are some

centimeters wide (Fig. 5c). The altered veins have indistinct boundaries to the host rock, and the morphology suggests that the leucogranite was ductile when the veins formed. Apart from the near absence of quartz and slightly coarser grain size, the mineral textures are similar to the other red leucogranites. In addition to unstable, heavily altered biotite, some euhedral biotite also occurs.

5 Zircon U-Pb

The BSE-images reveal that zircons in many samples are cracked and metamict. The internal heterogeneity of the zircons made it difficult to find suitable intact sites for analyses. However, combining concordia, upper intercept, and $^{207}Pb/^{206}Pb$ ages results in satisfactory ages. The results are presented as age diagrams along with examples of backscattered electron (BSE) images of analyzed zircons (Figs. 6 and 7). The complete analytical results are available in Electronic Appendix A.

5.1 Migmatites

5.1.1 Mellanskär quartz-feldspar paragneiss

The zircon grains in the megacryst-bearing quartz-feldspar paragneiss on Mellanskär (n5797, Fig. 1) are prismatic, subhedral, 200–400 µm long, and contain BSE-dark inclusions, some of which are Pb-rich (Fig. 6a). Many grains are heavily metamict. Eleven spots were analyzed on eleven grains. One zircon shows a very young 207Pb/206Pb age and is rejected. One grain shows an older concordant 207Pb/206Pb age of 1925 ± 24 Ma (2 sigma) and another is reversely discordant. The remaining eight analyses yield a concordia age of 1893 ± 6 Ma (2 sigma; MSWD=0.29). A weighted average 207Pb/206Pb age of 1892 ± 5 Ma (2 sigma; MSDW=0.73) obtained by using also the reversely discordant analyses in the calculation, is considered the best estimate for the crystallization age of the rock (Fig. 6a). As most of the zircons in the sample yield similar ages, a volcanic or volcaniclastic origin is more likely than sedimentary.

5.1.2 Mellanskär granitic metatexite

The zircons found in the granitic metatexite sample from Mellanskär (n5798, Fig. 1) are prismatic and up to 500 µm long (Fig. 6b). Sixteen analyses on sixteen grains form a cluster of twelve concordant/near-concordant, two discordant and one reversely discordant analyses, as well as two older data points with a mean 207Pb/206Pb age of 1923 ± 14 Ma (2 sigma). The cluster of twelve data points yields a concordia age of 1886 ± 4 Ma (2 sigma, MSWD=0.37).

5.1.3 Segelskär granitic metatexite

The zircon grains in the granitic metatexite from Segelskär (n5802, Fig. 1; Fig. 4a) are mostly prismatic, subhedral, 100–500 µm long and contain inclusions. Some grains have BSE-light homogenous rims around the heterogeneous cores (Fig. 6c). The data comprise 17 analyses, which form two clusters on the concordia line. Two analyses are discordant and omitted from the calculations. The older cluster comprises eleven analyses, but two of them are slightly younger than the main population. Nine analyses yield a concordia age of 1882 ± 4 Ma (2 sigma, MSWD=0.77), a similar weighted average 207Pb/206Pb age of 1881 ± 5 Ma (MSDW=1.16) and mean Th/U ratio of 0.34. The younger cluster comprises three slightly discordant and reversely discordant analyses. Their weighted average 207Pb/206Pb age is 1826 ± 5 Ma (2 sigma, MSDW=2.8) and mean Th/U ratio 0.05. Assuming that the lower Th/U ratio is related to metamorphic recrystallization (e.g., Kirkland *et al.* 2015), the older age represents the crystallization age of the granitic protolith whereas the younger age represents the migmatization event. This is supported by the BSE-images, which display overgrowths on older grains. Three analyses show 207Pb/206Pb ages of c. 1.87–1.84 Ga and Th/U

ratios of 0.31–0.16. These are core ages surrounded by younger rims and are regarded as mixed ages and therefore omitted from calculation.

5.1.4 Spikarna in-source leucosome

The Spikarna leucosome (n5796, Fig. 1) is an in-source leucosome from a megacryst-bearing quartz-feldspar paragneiss. The leucosome data set consists of 22 mostly subhedral, 100–400 µm long zircons that contain numerous inclusions. The data show discordant (n=4; two most discordant rejected) and concordant/near-concordant analyses (n=18) (Fig. 6d). The concordant data form two groups: an older one around 1.89 Ga (n=14), and a younger one around 1.82 Ga (n=3) as well as one analysis in between the two, which yields a 207Pb/206Pb age of 1845 ± 24 Ma (2 sigma). We consider this a mixed age and omit it. The older group consists of concordant and a few slightly discordant analyses that have a mean Th/U ratio of 0.33 and are likely to represent the volcanic protolith age. The concordant analyses also show a slight scatter along the Concordia line. Therefore, the weighted average 207Pb/206Pb age of 1888 ± 5 Ma (2 sigma, MSWD=0.68) is considered the best estimate for the crystallization age of the volcanic or volcaniclastic protolith. The younger population gives a concordia age of 1820 ± 5 Ma (2 sigma, MSWD=0.66) and has a mean Th/U ratio of 0.04, likely representing the migmatization event. Two of these analyses are from rims and the third from a zircon fragment without obvious zoning.

5.1.5 Mellanskär leucocratic dike

The Mellanskär leucocratic dike (n5799, Fig. 1) is hosted by both quartz-feldspar paragneiss and granitic metatexite. The sample contains very metamict grains with plenty of BSE-dark and bright inclusions and, consequently, it is difficult to find intact domains (Fig. 6e). Eight spots on eight grains are discordant or reversely discordant. The youngest analysis is extremely discordant and high in common Pb and consequently rejected. The oldest discordant analysis shows a likely inherited 207Pb/206Pb age of 1922 ± 17 Ma (2 sigma; not shown). The six analyses closest to the concordia yield an upper intercept age of 1818 ± 5 Ma (95% conf., MSWD=1.3) and a coherent 207Pb/206Pb weighted average age of 1821 ± 4 Ma (2 sigma, MSWD=1.8). The mean Th/U ratio of the six least discordant analyses is 0.05. Because of discordance, we prefer the 207Pb/206Pb age as the best estimate of the formation age of the leucocratic dike.

5.2 Even-grained granodiorite

The even-grained granodiorite from Lappohja (n5800, Fig. 1; Fig. 4d) contains rounded, 100–300 µm long zircons with deformed internal textures and inclusions. Despite only aiming for analysis sites at the least deformed parts of the grains, the five analyzed zircons were U-rich and affected by Pb-loss. Thus, the sample yielded no concordant ages, and we chose not to plot the results in a diagram. An upper intercept age of 1875 ± 10 Ma can, however, be discerned based on two analyses, and is cautiously considered the best age estimate for the rock.

5.3 Leucogranites

5.3.1 Bengtskär

The grey leucogranite on Bengtskär (n5793, Fig. 1) contains small (<200 µm long) zircons with inclusions (Fig. 7a). All the grains are partially metamict. Some of the zircons are euhedral and some of them appear to be fragments of larger grains. Seven analyses on five zircons show two concordant and five discordant analyses. Omitting the most discordant analysis, an upper intercept of six analyses yields an age of 1845 ± 9 Ma (95% conf., MSWD=0.7). The two concordant analyses give a concordia age of 1854 ± 10 Ma (2sigma, MSWD=0.26). Thus, a crystallization age of c. 1.85 Ga is the best estimate for this sample.

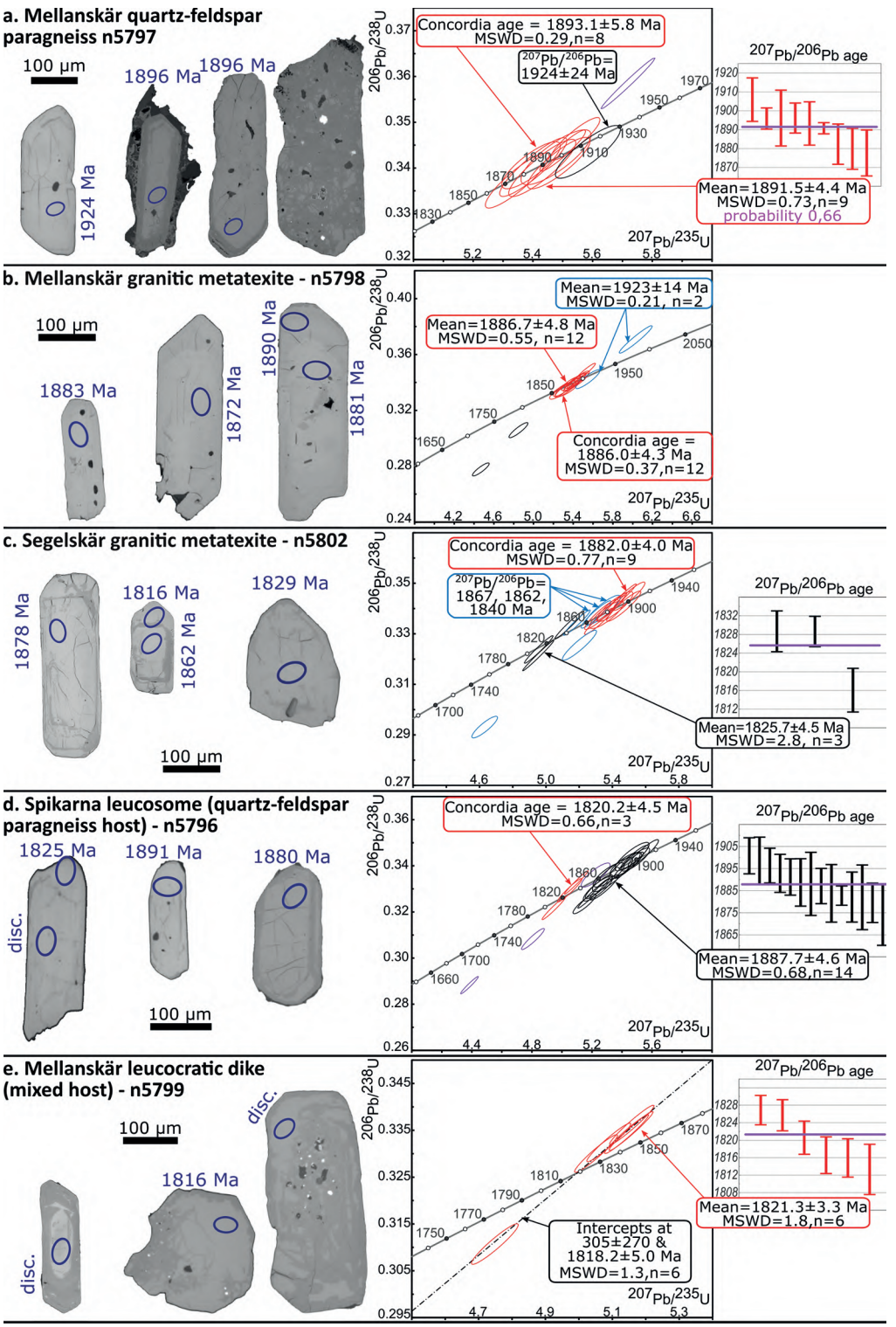

Fig. 6. BSE microscope images of representative zircons and concordia diagrams for the migmatite samples. Error symbols and bars at 1σ. Concordia and mean age errors at 2σ. Intercept age with 95% confidence. The ages depicted on the BSE images are 207Pb/206Pb ages.

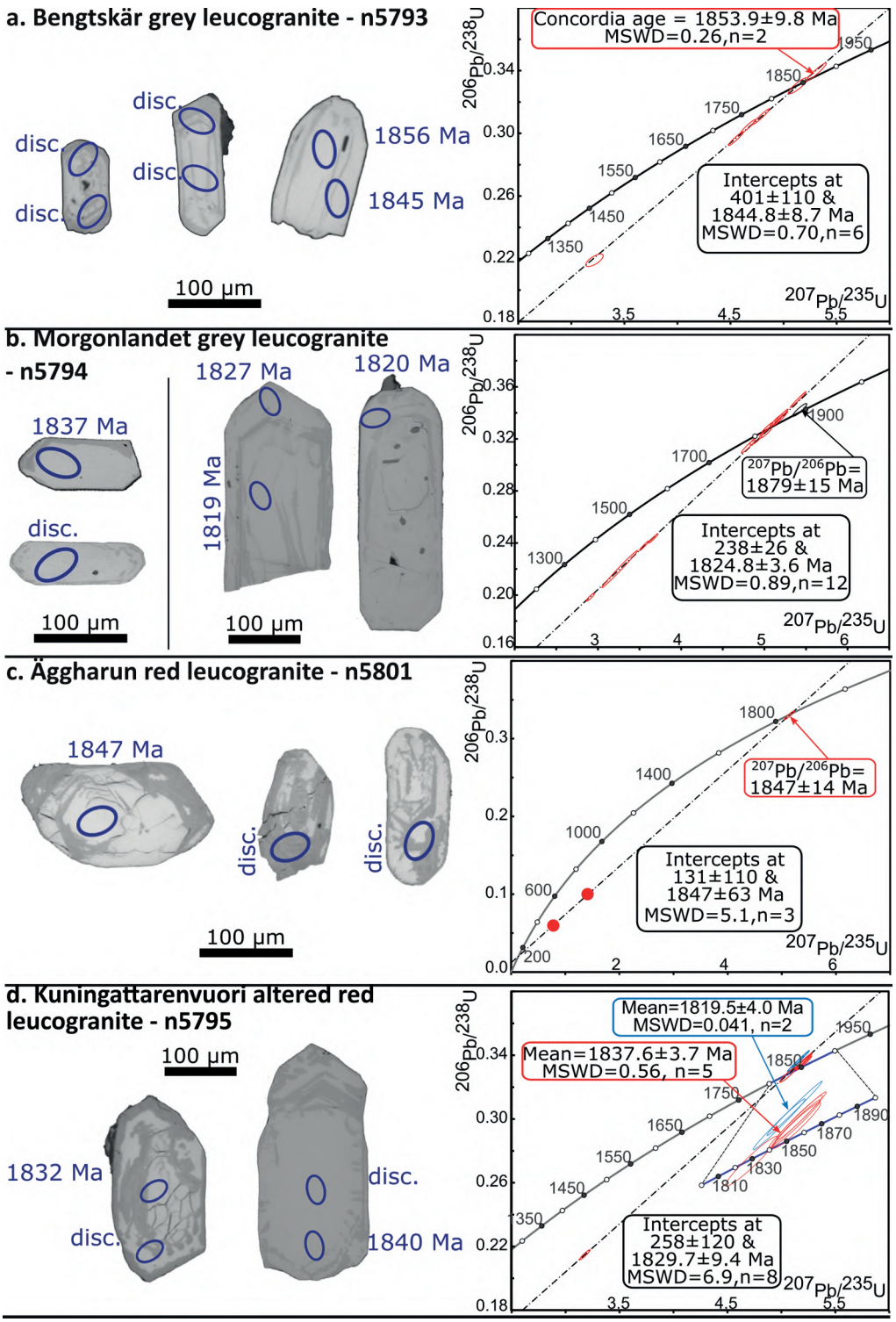

Fig. 7. BSE microscope images of representative zircons and concordia diagrams for the leucogranite samples. Error symbols at 1σ. Concordia and mean age errors at 2σ. Intercept ages with 95% confidence. The ages depicted on the BSE images are 207Pb/206Pb ages. c) The two discordant ages are marked with dots instead of error ellipses, because the errors are smaller than the dots, and thus difficult to distinguish.

5.3.2 Morgonlandet

The grey leucogranite on Morgonlandet (n5793, Fig. 1; Fig. 5a) contains partly metamict zircons, some of which are fragments. Most of the zircons are small, <200 µm long and contain inclusions and some zoning (Fig. 7b). 17 spots on 16 grains were analyzed. Most of the analyses are discordant or reversely discordant. One grain yields an older 207Pb/206Pb age of 1879 ± 15 Ma (2 sigma). Omitting the older one and the four most discordant analyses, an upper intercept age of 1825 ± 4 Ma is obtained (95% conf., MSWD=0.89).

5.3.3 Äggharun

The red leucogranite sample from Äggharun (n5801, Fig. 1) only contains a few subhedral, <200 µm long, cracked and metamict zircons (Fig. 7c). Out of three analyses, two are high in common lead and are very discordant, giving an unprecise upper intercept age of 1847 ± 63 Ma (MSWD=5.1). One of the analyses is concordant with a 207Pb/206Pb age of 1847 ± 14 Ma (2 sigma), which is regarded as the best age estimate for this rock, although it should be treated with caution.

5.3.4 Kuningattarenvuori

The altered Kuningattarenvuori leucogranite (n5795, Fig. 1; Fig. 5c) contains few zircons, some of which are metamict (Fig. 7d). They are subhedral and 200–400 µm long. Eight spots on six zircons yield one discordant point and a cluster of seven slightly reversely discordant analyses. All eight analyses give an upper intercept age 1830 ± 10 Ma (95% conf., MSWD=6.9). The seven slightly reversely discordant analyses form two small adjacent clusters. The older cluster (n=5) yields a 207Pb/206Pb age of 1838 ± 4 Ma (2 sigma, MSWD=0.56) and the younger cluster (n=2) yields a 207Pb/206Pb age of 1820 ± 4 Ma (2sigma, MSDW=0.041). The younger analyses show lower Th/U ratios (mean 0.03) compared to the older ones (mean 0.16), indicating that the older age is the crystallization age and the younger one an event of metamorphic recrystallization.

6 Whole-rock geochemistry

6.1 Major elements

The whole-rock major element analytical results for representative samples of each rock type are shown in Table 2, and the full results for all samples in Electronic Appendix B.

In the TAS classification diagram (Fig. 8a; Middlemost 1994) all leucosomes and leucogranites are silica-rich (>70 wt.% SiO_2) granites *sensu stricto*. There is no systematic compositional variation between the red and grey leucogranites, so we discuss them as a single group. The even-grained granitoids (n5800 and MJV-samples; Fig. 4d) from the mainland plot in the granodiorite and granite fields, so to distinguish them from the other granitoids in this study, we continue to refer to them as granodiorites. The granitic metatexites (n5798 and n5802; Fig. 3c and Fig. 4a) partly overlap with the granodiorites but are generally more K-rich. For comparison, we plot the orthoclase megacryst-bearing quartz-feldspar paragneisses (n5797; Fig. 3c) in the TAS diagram, although their current compositions should not be assumed to fully reflect their original compositions due to the feldspar crystallization and anatectic processes they have experienced. They are compositionally similar to the granitic metatexites but display a wider variation in SiO_2-content. The altered leucogranite on Kuningattarenvuori (n5795; Fig. 5c, d) is geochemically a syenite, displaying much higher alkali and lower silica contents than the normal leucogranites.

The feldspar triangle based on CIPW normative compositions of the leucosome samples (Fig. 8b), shows that all the leucosomes contain significant amounts of K-feldspar, and are thus classified as granites.

The general geochemical characteristics for the granitoids and metagranitoids are shown in Figs.

Table 2. Major element composition of representative samples. Coordinates in ETRS-TM35FIN

ID	Migma-2016-26.1	Migma-2016-52.2	Migma-2016-26.2 (n5798)	Migma-2016-47.2	Migma-2015-25 (n5800)	19-MJV-07	Migma-2015-20
N	6637807	6634758	6637761	6630685	6646836	6648116	6636571
E	289712	298987	289656	296417	289438	292287	287440
Site	Mellanskär	Stenskär	Mellanskär	Segelskär	Lappohja	Hangövägen	Spikarna E
Rock type	Quartz-feldspar paragneiss	Quartz-feldspar paragneiss	Granitic metatexite	Granitic metatexite	Even-grained granodiorite	Even-grained granodiorite	Leucosome or felsic dike
Laboratory	ActLabs	ActLabs	ActLabs	ActLabs	Geohouse	AcmeLabs	Geohouse
wt.%							
SiO_2	73.87	61.93	66.28	70.83	73.16	66.49	73.85
TiO_2	0.23	0.42	0.69	0.42	0.23	0.82	0.12
Al_2O_3	13.87	16.55	15.53	13.60	13.81	15.35	13.06
Fe_2O_3	b.d.l.	1.24	0.61	0.99	n.a.	n.a.	n.a.
FeO	2.30	4.70	5.10	2.30	n.a.	n.a.	n.a.
Fe_2O_3t	2.55	6.47	6.28	3.55	2.35	n.a.	1.62
FeOt	n.a.	n.a.	n.a.	n.a.	n.a.	4.84	n.a.
MnO	0.04	0.10	0.08	0.05	0.02	0.05	0.01
MgO	0.37	1.18	0.94	0.60	0.58	1.57	0.26
CaO	2.62	4.47	3.33	1.00	1.63	3.45	0.26
Na_2O	3.55	3.37	3.65	2.32	2.90	3.41	1.74
K_2O	2.04	5.28	2.59	5.78	4.61	2.40	7.75
P_2O_5	0.04	0.24	0.20	0.10	0.06	0.28	0.01
LOI	0.27	0.80	0.50	0.67	0.04	0.60	0.49
LOI2	0.01	0.27	b.d.l.	0.41	n.a.	n.a.	n.a.
Total oxides	99.45	100.80	100.10	98.91	99.36	99.84	99.17

ID	Migma-2016-50.2	Migma-2016-60.3	Migma-2017-9.1 (n5794)	Migma-2015-28	Migma-2016-53.1 (n5801)	Migma-2017-1.1B (n5795*)
N	6634075	6629245	6632601	6638283	6636873	6638206
E	297986	246882	258754	273595	295406	273594
Site	Klovaskär	Bengtskär	Morgonlandet	Hanko	Äggharun	Kuningattarenvuori
Rock type	Leucosome or felsic dike	Grey leucogranite	Grey leucogranite	Red leucogranite	Red leucogranite	Altered leucogranite
Laboratory	ActLabs	ActLabs	ActLabs	ActLabs	ActLabs	ActLabs
wt.%						
SiO_2	72.93	73.08	71.60	73.28	74.84	63.37
TiO_2	0.26	0.16	0.26	0.12	0.12	0.23
Al_2O_3	13.41	13.60	13.74	13.55	13.45	17.28
Fe_2O_3	0.12	0.17	0.17	0.07	0.27	0.22
FeO	2.10	1.20	1.80	1.60	1.70	2.30
Fe_2O_3t	2.46	1.50	2.17	1.85	2.16	2.77
FeOt	n.a.	n.a.	n.a.	n.a.	n.a.	n.a.
MnO	0.03	0.03	0.04	0.06	0.06	0.04
MgO	0.49	0.25	0.39	0.23	0.32	0.34
CaO	1.51	0.90	1.19	1.22	1.27	1.00
Na_2O	2.38	2.09	2.55	2.72	2.58	3.02
K_2O	5.85	6.61	5.94	5.36	5.06	9.63
P_2O_5	0.07	0.03	0.04	0.01	0.03	0.07
LOI	0.61	0.77	0.56	0.54	0.62	0.64
LOI2	0.38	0.64	0.36	0.36	0.43	0.39
Total oxides	100.00	99.02	98.48	98.95	100.50	98.41

* Only the altered portion of the sample used for geochemical analysis, zircons for dating picked from a sample containing both altered and unaltered portions.

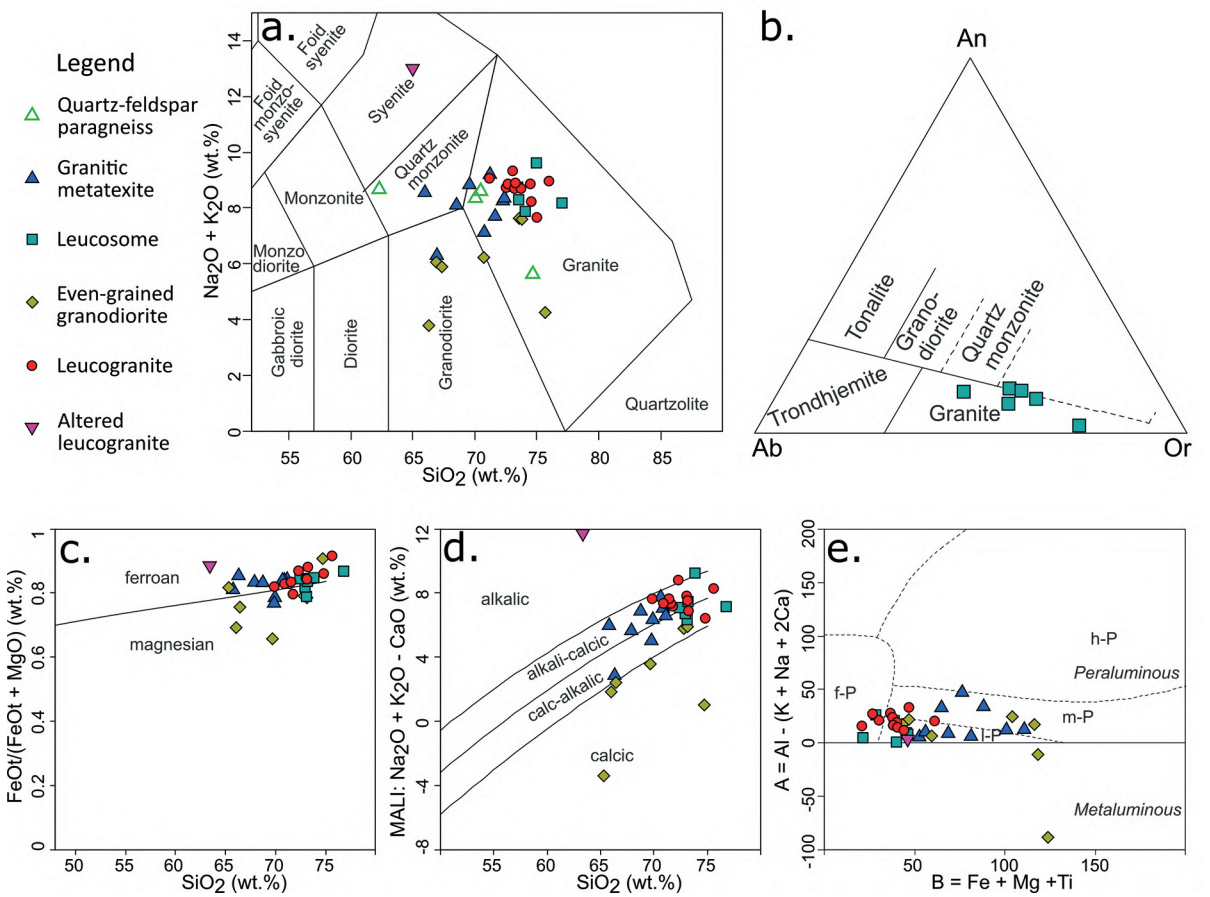

Fig. 8. Major element diagrams: a) TAS diagram for all samples (Middlemost 1994), b) Feldspar triangle for leucosome samples (O'Connor 1965), c) Ferroan-magnesian division (Frost & Frost 2008), d) Alkalic-calcic division (Frost & Frost 2008), e) B-A diagram (Villaseca et al. 1998).

8c, d, loosely following the classification system for feldspathic igneous rocks by Frost & Frost (2008). In the ferroan-magnesian division, the granitic metatexites and leucogranites are mainly ferroan, whereas the even-grained granodiorites are mostly magnesian. Leucosomes straddle the dividing line evenly. The even-grained granodiorites are distinctly calcic, whereas the granitic metatexites, leucogranites and leucosomes are calc-alkalic to alkali-calcic. The Kuningattarenvuori altered leucogranite is significantly more alkalic than any other rocks.

Apart from some of the even-grained granodiorites, which are metaluminous, all our analyzed samples are weakly peraluminous (Fig. 8e). Although leucogranites in general tend to be highly felsic peraluminous (Villaseca *et al.* 1998), only a few of the leucogranite samples plot into that field. As biotite is the only mafic mineral present in the granitic metatexites, leucosomes, and red leucogranites in any substantial quantity, the mafic components iron and magnesium directly reflect the biotite content in the samples. Granitic metatexites contain more mafic components than the leucosomes or leucogranites, whereas total alkali is similar among the rock types. The iron-to-magnesium ratio is the same in metatexites, leucosomes, and leucogranites. The even-grained granodiorites differ from the other rocks in that they contain a larger variation in the mafic components.

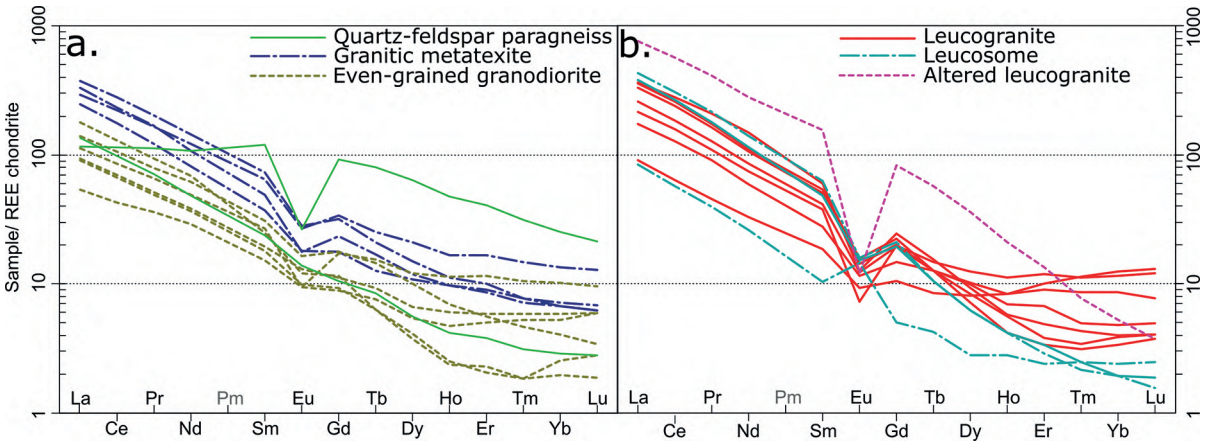

Fig. 9. Chondrite-normalized (Boynton 1984) REE diagrams for a) quartz-feldspar paragneiss, granitic metatexite and even-grained granodiorite. The trends of the granitic metatexites and even-grained granodiorites are similar, but the granitic metatexites contain more REE. The HREE contents vary more than LREE. b) leucogranites and leucosomes. The leucogranites follow a similar general trend as the metatexites and granodiorites. One of the leucosomes displays a positive Eu peak that likely indicates early crystallizing plagioclase in the partial melt, whereas the two others have compositions similar to the leucogranites.

6.2 Trace elements

Chondrite normalized REE diagrams (Fig. 9, normalization values after Boynton (1984)) show that the even-grained granodiorites, granitic metatexites, and leucogranites have similarly shaped patterns, but all the REE are slightly more enriched in the granitic metatexites than in the even-grained granodiorites. The leucogranite REE compositions are generally similar to the granitic metatexites but display a larger internal variation. The altered leucogranite on Kuningattarenvuori displays higher REE contents than the regular leucogranites, except for Eu and the heaviest REE (Tm, Yb, Lu). Two of the three leucosomes follow the same pattern as the leucogranites, but one (Migma-2016-48.3) displays a positive Eu anomaly and lower LREE contents. The REE contents of the two analyzed quartz-feldspar paragneisses are dissimilar to each other, and to the granitic metatexites. The altered leucogranite at Kuningattarenvuori is heavily enriched in LREE as well as Th, U, and Rb.

Because accessory minerals are associated with biotite in the migmatites and leucogranites, we plotted some minor and trace elements occurring in such accessory minerals against biotite components FeOt+MgO to identify trends (Fig. 10). P_2O_5, Zr, and Hf correlate with FeOt+MgO, and are thus mostly depleted in the leucogranites and leucosomes in comparison to the metatexites. These elements are significant constituents of apatite and zircon, accessory minerals often found as inclusions within biotites or biotite clusters in our thin sections. Elements compatible with monazite (Rb, Th, U, and light REE) are present in roughly similar quantities in all the rock types, although the variation is a little higher among the leucosomes and leucogranites than among the metatexites, corresponding to the observed mineralogy with monazite found in all rock types.

7. Discussion

7.1 Early Svecofennian magmatism

Early Svecofennian volcanism is visible in the study area as the metamorphic rocks that have their origins in volcanic layers and volcanogenic sediments. The strongly migmatized quartz-feldspar paragneisses represent intermediate to felsic volcanic material, whereas the less melted

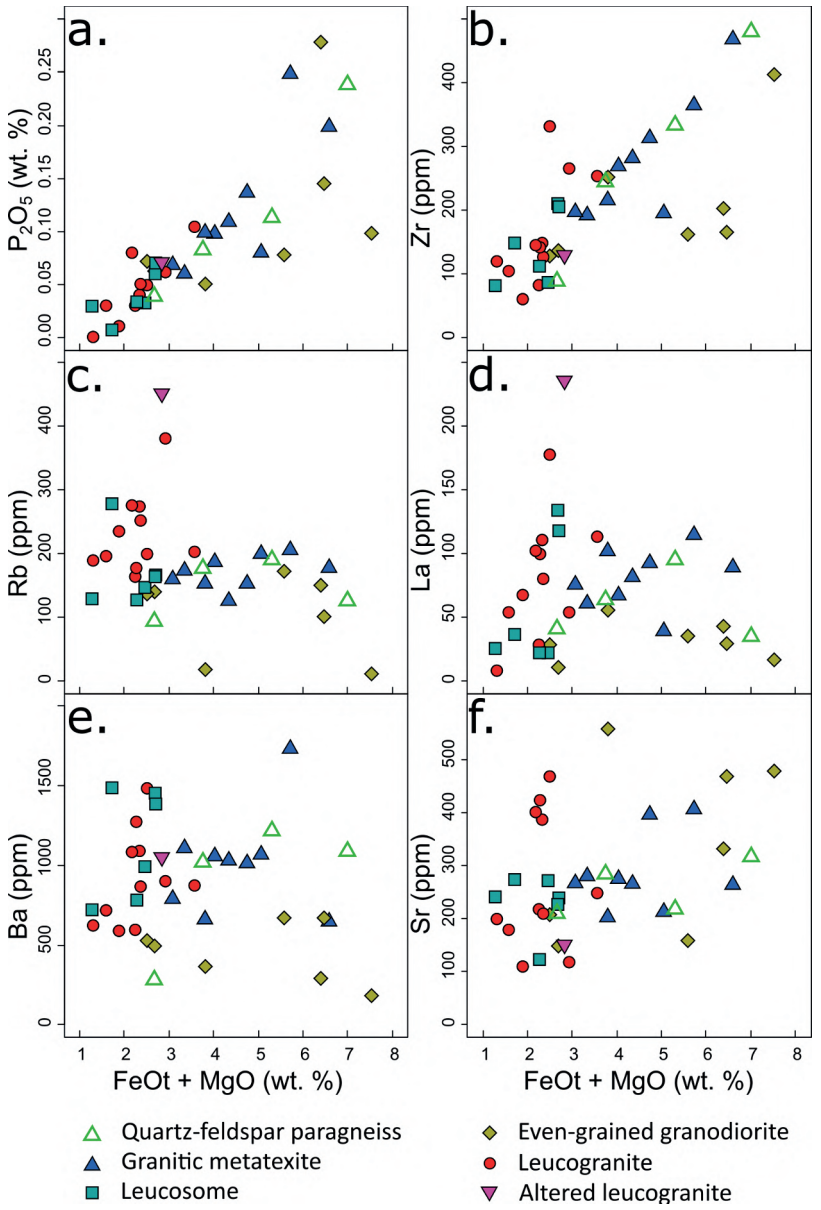

Fig. 10. Minor or trace element concentrations against FeOt+MgO. a-b) P and Zr are more abundant in the metatexites and granodiorites than in leucogranites. Other elements displaying similar trends are Y, Hf, and Eu. c-d) In the leucogranites, Rb and La occur in concentrations similar to or slightly higher than those of the metatexites and granodiorites. Ce, Nd, and Th display similar behavior. e-f) Ba and Sr show no systematic variation between the rock types.

amphibolites are remnants of mafic layers. This volcanism took place at around 1.90–1.88 Ga, as evidenced by the analyzed quartz-feldspar paragneiss age and inherited zircon age from a leucosome in a quartz-feldspar paragneiss, as well as amphibolitic migmatite ages in the northwest of the area (Bredenberg 2019).

Granitoid magmatism during the early Svecofennian is represented by two distinct rock types in our study area: the granitic metatexites, and the even-grained granodiorites, both of which have been affected by the late Svecofennian events and thus predate the late migmatization and leucogranite formation (Fig. 11). The most

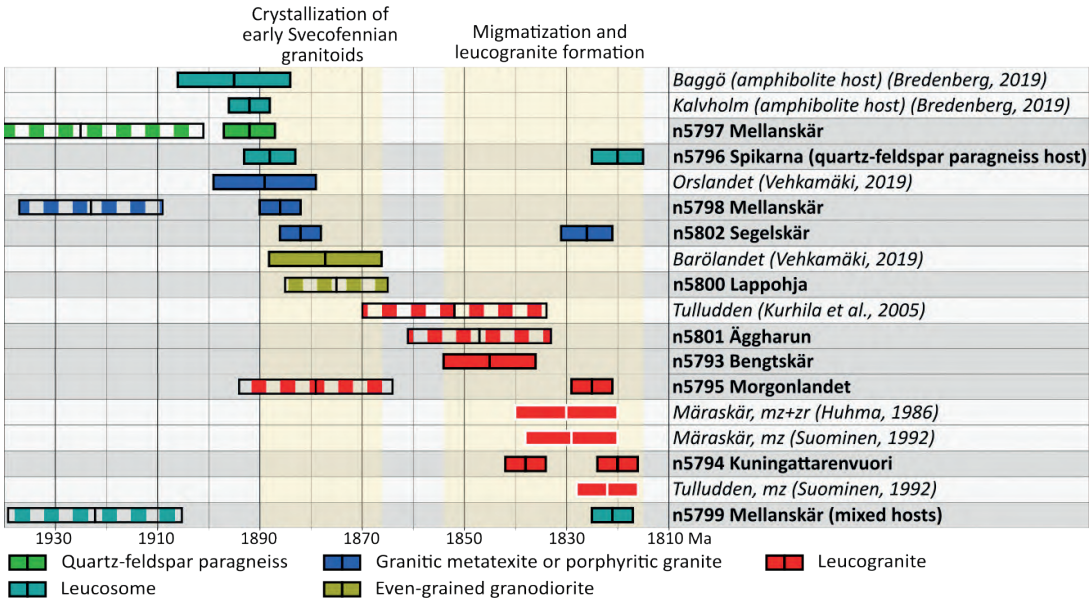

Fig. 11. Summary of U-Pb age data from the study area and proposed granitoid formation events. For legibility, the reference data rock types have been renamed to correspond with the rock type classification system used in this paper. Boxes with hatched filling represent age data with limited reliability. Black edges around boxes denote zircon analyses, white edges monazite analyses.

obvious difference between these two rock types is that unlike the even-grained granodiorites, the granitic metatexites contain abundant K-feldspar megacrysts – a distinction also visible in geochemical compositions as the higher K-content of the granitic metatexites (Fig. 12). The granitic metatexites are also visibly mylonitic, indicating shearing in many locations, whereas deformation in the even-grained granodiorites is only schistose (Fig. 4a, d). The even-grained granodiorite from Lappohja has an uncertain, slightly younger but partly overlapping, age estimate compared to the granitic metatexites, and as we did not find these rock types on the same outcrops, we could not reliably determine their relative ages. Outside the study area, Vehkamäki (2019) and Ehlers et al. (1993) have found tonalites and granodiorites that are slightly younger than the other early Svecofennian rocks, making it plausible that the even-grained granodiorites crystallized shortly after the protolith of the granitic metatexites. Alternatively, they can represent the same granitoid suite at different degrees of partial melting or alteration, so there does not need to be a systematic age difference.

Arc-related tonalite-trondhjemite-granodiorite-like magmatism at 1890–1880 Ma is found in many locations throughout the Svecofennian, such as the Bergslagen lithotectonic unit 1.91–1.87 Ga (1.91–1.87 Ga; Stephens & Jansson 2020), the Central Finland Granitoid Complex (Nironen 2003; Nikkilä *et al.* 2016), and Orijärvi and Enklinge (Väisänen *et al.* 2012b; Kara *et al.* 2018). Many early Svecofennian granitoids were intruded along or with the help of shear zones (e.g., Nikkilä *et al.* 2016; Torvela & Kurhila 2022). Also, the granitic metatexites in southernmost Finland are associated with shear zones (Fig. 2), indicating that their granitoid protolith likely intruded through shear zones at 1890–1880 Ma.

Early Svecofennian granitoids elsewhere in the domain are compositionally different from the granitic metatexites in the Hanko-Ekenäs area, but largely similar to the even-grained granodiorites

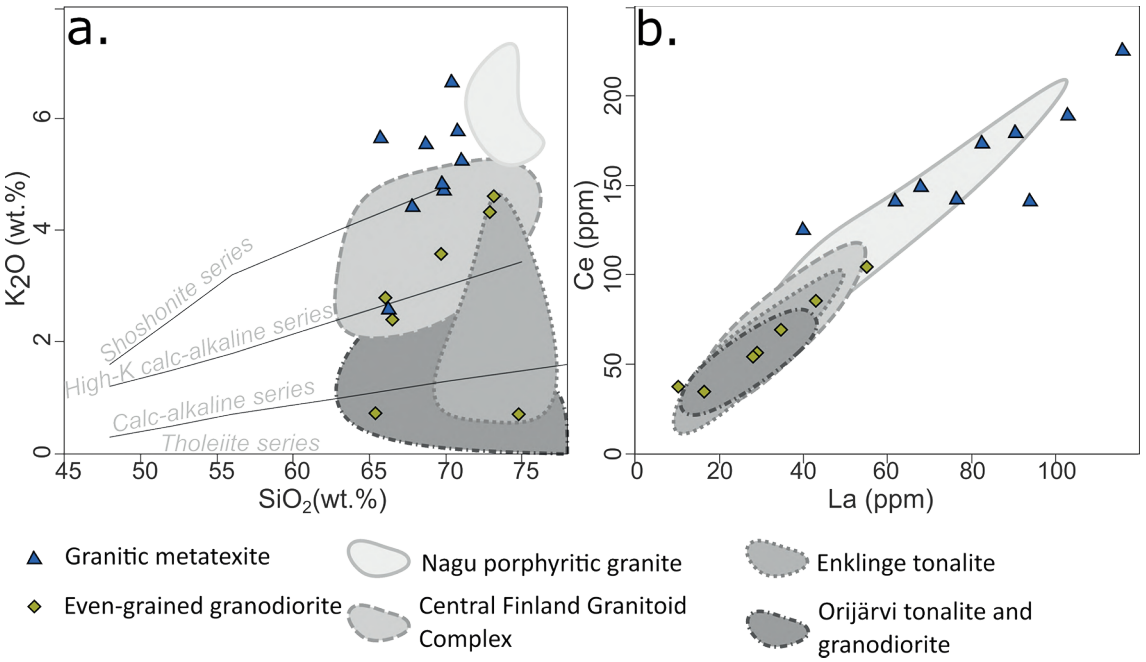

Fig. 12. Early Svecofennian granitoids from Orijärvi and Enklinge in the Southern Finland Subprovince (Kara *et al.* 2018) and the Central Finland Granitoid Complex (Nikkilä *et al.* 2016). The porphyritic Nagu granite (Stålfors & Ehlers 2006) is included because of its proximity and mineralogical similarity to the granitic metatexites, even though it has not been classified as an early Svecofennian granite. a) SiO2-K2O diagram (Peccerillo & Taylor 1976) shows that the even-grained granodiorites are similar to TTG-like rocks in Orijärvi and the Central Finland Granitoid Complex, whereas the granitic metatexites are generally more K-rich. The Nagu porphyritic granites are similar to the granitic metatexites in K-content but are more SiO2-rich. b) The LREE contents, here exemplified by La and Ce, of the granitic metatexites are higher than those of the even-grained granodiorites and most reference data, apart from the Nagu porphyritic granite.

(Fig. 12). The granitic metatexites in our study area contain more potassium and LREE compared to the even-grained granodiorites, the TTG-like rocks in Orijärvi and Enklinge (Väisänen *et al.* 2012b; Kara *et al.* 2018), and the granitoids in the Central Finland Granitoid Complex (Nikkilä et al 2016). They have, however similar silica contents and La-to-Ce-ratios. The closest compositional match to the granitic metatexites are the porphyritic Nagu granites (Stålfors & Ehlers 2006), which also contain K-feldspar megacrysts. However, the Nagu granites are more silica rich, and the K-felspar megacrysts they contain consist of microcline (Stålfors & Ehlers 2006), whereas those in our study area consist of orthoclase displaying some degree of microclinitization. Altogether, the potassium content appears to be directly reflected by the presence of K-feldspar megacrysts.

7.2 Crystallization of K-feldspar megacrysts

As the conspicuous K-feldspar megacrysts and the corresponding high K-content in the granitic metatexites distinguish them from other early Svecofennian granitoids, including the even grained granodiorites of the study area, untangling the origins of the megacrysts is important. K-feldspar megacrysts in granitoids often have igneous rather than metamorphic or metasomatic origins (e.g., Vernon & Paterson 2002), so it is plausible that the protolith to the granitic metatexite was K-rich already as it intruded and the megacrysts are a primary feature. This is also tentatively supported by weak zoning in the megacrysts and inclusions that display no preferred orientation. However, the megacrysts in the neighboring, originally

supracrustal units (Fig. 3b, c) are more difficult to reconcile with an igneous origin.

Apart from crystallization in mostly liquid magmas, another mechanism that can produce K-feldspar megacrysts is thermal cycling, where the textural coarsening of K-feldspars takes place in nearly solid environments during separate pulses of magma emplacement (Johnson & Glazner 2010). New magma batches cause reheating of and fluid influx into their surroundings, making preexisting K-feldspar grow larger by each arriving batch. Although the model was developed for incrementally accrued granitoid plutons, the mechanism could work for any type of rock with suitable K-feldspar seeds subjected to reheating and fluid influx, such as the paragneisses in our study area. However, megacrysts growing through thermal cycling generally grow idiomorphic and in zones, whereas the paragneiss megacrysts are asymmetric and lack zoning. This suggests that they are porphyroclasts, or were later deformed so heavily that the original features were obscured.

The sizes and amount of megacrysts in the originally supracrustal rocks increase with proximity to both shear zones and the granitic metatexites (Fig. 2b). As the protolith to the granitic metatexite intruded along the shear zones, it may have released K-rich co-magmatic fluids and heat that altered the surroundings. Alternatively, the shear zones could have introduced K-rich fluids to both the paragneiss and the granitoids. Shear zones are commonly thought to act as fluid channels (e.g., Dipple & Ferry 1992; Bucholz & Ague 2010), and they may have channeled the metasomatic fluids also in southern Finland. In magmatic arcs, potassic fluids are derived from the subducting slab at shallow depths (Massonne 1992), whereas deep potassic fluids mostly come from mantle sources (Jarrard 2003). Fluid influx would explain the unusually high K-content of the granitic metatexite compared to other early Svecofennian granitoids not as a primary feature but resulting from later alteration. However, unless the shear zones were reactivated multiple times, this is difficult to reconcile with the porphyroclasts. Regardless of whether the fluid influx was co-magmatic or not, the changes in chemical composition caused by metasomatism were significant for the later stages of bedrock evolution in the study area.

No evidence of early Svecofennian K-metasomatism has also been found elsewhere in the orogen. However, Stephens & Jansson (2020) described a metasomatic event that altered some of the c. 1910–1870 Ma granitoid plutons in the Bergslagen lithotectonic unit prior to the metamorphic peak at 1870–1860 Ma. In Bergslagen, the rocks were depleted in K-feldspar and enriched in quartz and albite components, whereas the metasomatically altered rocks in our study area are enriched in potassium and depleted in silica. As Bergslagen and Southern Finland have been thought to form a single crustal unit (Lahtinen *et al.* 2005), the metasomatic events in southernmost Finland and Sweden may be related, although the types of fluid alteration are different.

7.3 Late Svecofennian partial melting and leucogranites

The late Svecofennian partial melting event that formed the migmatites and leucogranites occurred over a long period of time, from 1850 to 1790 Ma in the southern Finland Subprovince (Huhma 1986; Kurhila *et al.* 2005, 2011) and around 1840 to 1810 Ma in central Sweden (Stephens & Jansson 2020). In our study area, the ages span from around 1855 to 1815 Ma, although the upper age limit remains imprecise. It is possible that partial melts were present and leucogranites crystallized continuously for the entire 40-Myr-long period as suggested by the monazite age results by (Huhma 1986; Suominen 1991), or occurred in multiple pulses as proposed by Kurhila et al. (2005). Notably, our Kuningattarenvuori sample records two non-overlapping ages (1838 ± 4 Ma and 1820 ± 4 Ma), the older likely representing the original crystallization age and the younger an overprint that coincided with leucosome crystallization in migmatites. The Korpo granite to the west of the study area also contains two

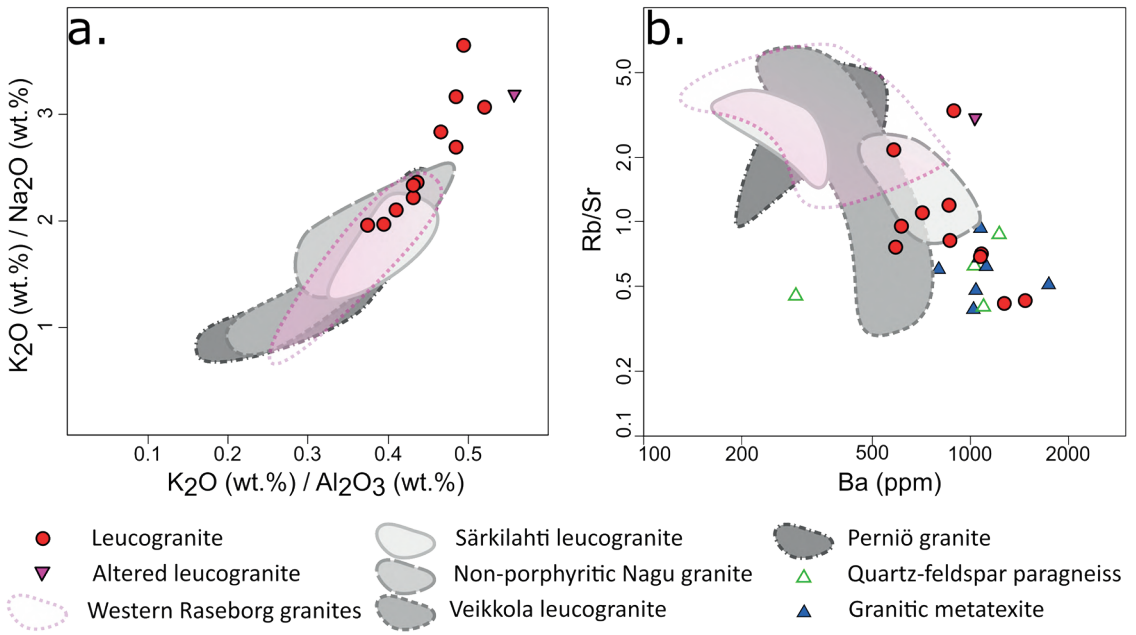

Fig. 13. Southernmost Finland leucogranites compared to other Svecofennian leucogranites (Stålfors & Ehlers 2006; Nironen & Kurhila 2008; Geological Survey of Finland 2014; Mäkitie *et al.* 2019). a) High potassium-to-sodium and potassium-to-aluminum ratios distinguish the study area leucogranites from the reference data. b) The Rb-to-Sr ratio in most of the southernmost Finland leucogranites is similar to the migmatites, and there are fewer high-Rb samples than among the reference leucogranites. The Rb/Sr-ratio is particularly low in comparison to the Western Raseborg granites located immediately to the north of the study area.

non-overlapping ages (Väisänen *et al.* 2012a). This suggests that at least locally, the late Svecofennian zircon crystallization occurred in two pulses, corresponding to cyclic crustal melting and pluton construction processes also described in other regions (e.g., De Saint Blanquat *et al.* 2011; Wolfram *et al.* 2019).

Late Svecofennian leucogranites generally contain microcline as the most dominant feldspar, two micas, and abundant garnet (Kurhila 2011). Many migmatites and associated granites in the southern Finland Subprovince formed through dehydration melting (Mengel *et al.* 2001; Johannes *et al.* 2003; Andersen & Rämö 2021), a process also reflected by the high amounts of peritectic garnet (e.g., Brown 2013). In the western part of the Subprovince, metapelitic rocks are thought to have been the primary protolith of the migmatites and some of the granites (Mengel *et al.* 2001; Johannes *et al.* 2003), whereas Andersen & Rämö (2021) proposed that metaigneous rocks were more important as source rocks for the southern Finland leucogranites in general.

Compositionally, the study area leucogranites are different from most other late Svecofennian leucogranites in the subprovince (Fig. 13). Garnet only appears in minor amounts in some of the red leucogranites, and instead of microcline, the main feldspar is orthoclase – albeit partially microclinitized. Opaque minerals are common in the study area leucogranites, but near-absent elsewhere. Geochemically, the leucogranites we investigated have high K_2O/Na_2O and K_2O/Al_2O_3 ratios relative to the other leucogranites (Fig. 13a), although the partial overlap with data from the geographically nearby Nagu and Western Raseborg areas may indicate a gradual increase of K_2O in the protoliths, rather than an abrupt compositional difference.

The early Svecofennian megacryst-bearing

granitoids and metasupracrustal rocks are the main paleosome in migmatites and are also found as partially assimilated rafts in all study area leucogranites, indicating that they were the protoliths during the late Sveocfennian partial melting event. Furthermore, as the leucogranites and leucosomes are only slightly peraluminous, metapelitic sources can be ruled out (Villaseca *et al.* 1998), distinguishing the area from southwestern Finland (Mengel *et al.* 2001; Johannes *et al.* 2003).

In the Hanko-Ekenäs area, water-fluxed melting is indicated by leucosome morphology (Sawyer 2010; Weinberg & Hasalová 2015) and the presence of peritectic hornblende (Weinberg & Hasalová 2015; Fig. 4a). This indicates that in contrast to other migmatites in the Southern Finland Subprovince, the anatectic event in our study area started when water-rich fluids entered the crust. Rb-to-Sr ratio remaining the same between the source migmatites and melt product leucogranites is also consistent with water-fluxed melting (Fig. 13b), as Rb tends to increase in dehydration melting (Inger & Harris 1993). The difference to the Western Raseborg leucogranites (Geological Survey of Finland 2014) on the northern side of the Hitis shear zone is distinct. However, water-fluxed melting often produces tonalitic melts, which is in contrast with the granitic leucosomes in the study area (Fig. 8b), so further work is needed to better constrain the melting reactions in the area.

7.4 Bedrock evolution in the study area

The bedrock evolution in southernmost Finland started with deposition of volcanic and sedimentary material in a basin close to a magmatic arc (Hopgood *et al.* 1983; Hopgood 1984; Fig. 14a). The presence of thin carbonate rock interlayers suggests a marine environment (e.g., Ehlers *et al.* 1993). The maximum deposition ages of the sediments are poorly constrained, but we found no evidence of zircon populations older than ca 1920 Ma, and neither have earlier studies in the study area (Hopgood *et al.* 1983), although this may also reflect on the sparsity of data. This is in contrast to the rest of Southern Finland, where ca 2.0 Ga and Archean populations are common as inherited cores of zircons (Kurhila *et al.* 2011; Väisänen *et al.* 2012b; Kara *et al.* 2018; Lahtinen *et al.* 2022; Salminen & Kurhila 2024). As the investigated samples are mainly metavolcanic and metavolcaniclastic rather than metasedimentary, the lack of inherited older zircons can indicate that the majority of the zircons originate from the local volcanic activity. Zircon ages in originally supracrustal rocks (n5797, n5797; Bredenberg 2019) cluster around 1900–1880 Ma, indicating deposition and volcanism prior to and around the same time as the earliest Svecofennian granitoids intruded.

The early Svecofennian granitoids in the study area mostly appear as foliation-parallel intrusions among the older, originally supracrustal rocks (Fig. 14b). They come in two distinct types: granitic, K-feldspar megacryst-bearing rocks, and granodioritic, even-grained rocks. The megacryst-bearing granitoid and K-feldspar megacrysts found in paragneisses are associated with km-scale shear zones, so the crystallization of K-feldspar megacrysts appears related to the shear-zones. This may have occurred co-magmatically when the shear zones transported the granitoid magma, or later as an overprint (Fig. 14c).

Crustal fracture zones and local shear zones may have repeatedly acted as fluid conduits during the orogeny: the maximum age of the shear zones is the crystallization age of the thoroughly mylonitized granitic metaxite, ca 1880 Ma., and the minimum age is the age of the leucosomes crosscutting the mylonite, ca 1820 Ma. However, as no shear zones were found in the oldest leucogranites, the shear zone minimum age may be as old as 1850 Ma. Mylonite observations and bathymetric data suggest that in addition to the previously described E–W shear zones, at least one NNE-striking shear zone is also present in the area (Fig. 2b), as is common in the Subprovince (e.g., Torvela & Kurhila 2022; Nordbäck *et al.* 2023).

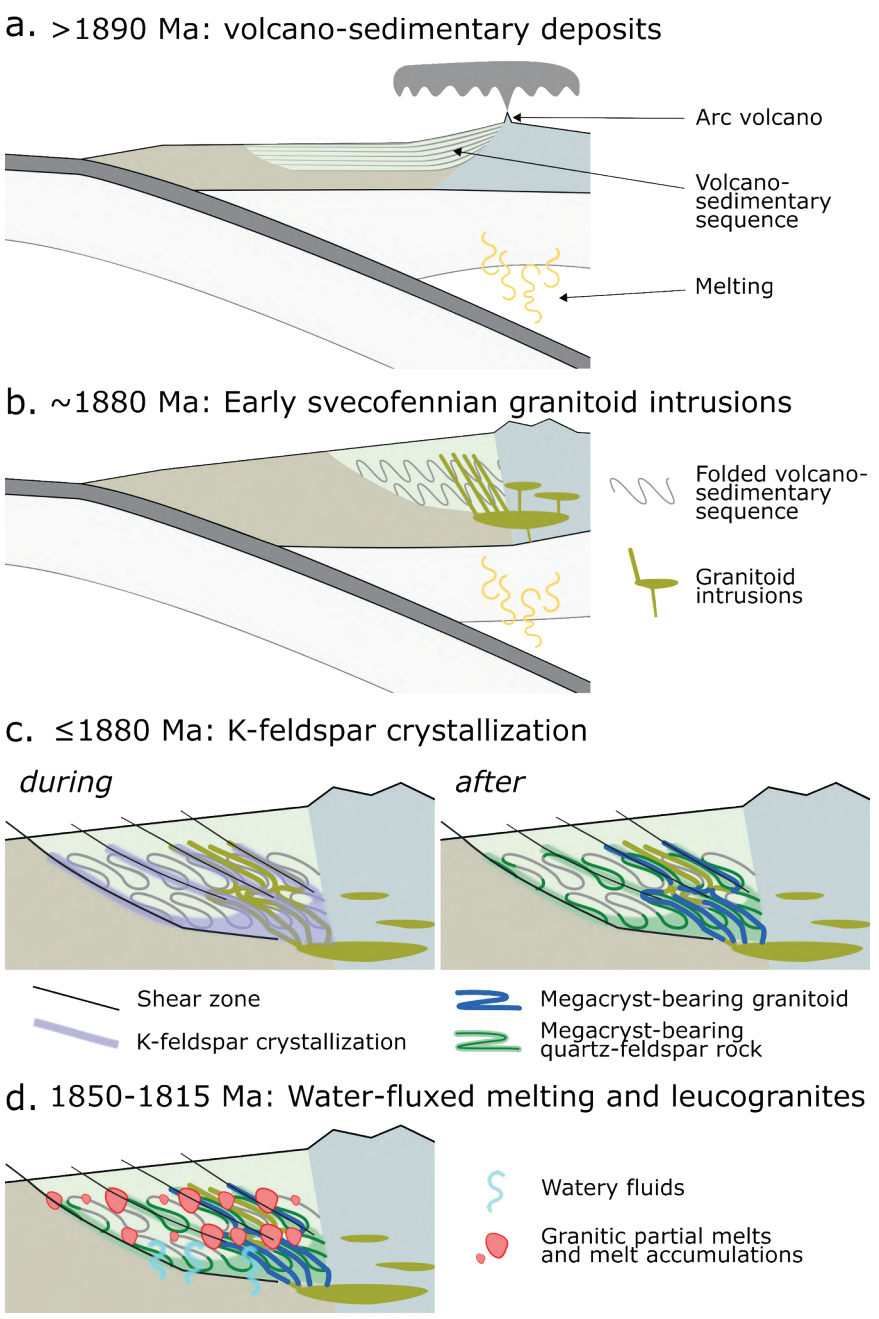

Fig. 14. Schematic interpretation of how the different granitoids and supracrustal rocks in southernmost Finland were formed and transformed. a) The Svecofennian orogeny began with volcano-sedimentary processes in a basin near a magmatic arc. b) As compression proceeded and folding of the basin material occurred, arc-related granodioritic magmas intruded parallel to the folds. c) Potassium feldspar crystallized in the rocks close to the shear zones. The crystallization mechanism is currently unknown but may have been due to heat pulses and co-magmatic fluids from some of the intruding granitoids, or occurred as a separate metasomatic event where the fluids moved through the shear zones. After the crystallization event, the originally supracrustal units contained K-feldspar megacrysts, and two types of early Svecofennian granitoids were present: the even-grained granodiorites and the megacryst-bearing granitoids. d) Influx of aqueous fluids initiated partial melting in the early Svecofennian rocks, turning them into migmatites and producing the leucogranites.

Fluid activity in the area was prevalent once again during migmatization and leucogranite formation at 1850–1815 Ma, when influx of water kick-started the melting reactions in the older granitoids and supracrustals (Fig. 14d). Whether these aqueous fluids were also channeled through reactivated shear zones is not known, but shear zone reactivation was common during the Svecofennian orogeny (e.g., Torvela & Kurhila 2022).

8 Conclusions

Several events of granitoid formation occurred in southernmost Finland during the Svecofennian orogeny, as evidenced by the new age data in this paper. The oldest granitoids in the study area intruded supracrustal rocks at around 1890–1870 Ma, and now appears as granitic metatexite. The even-grained granodiorite that formed at approximately the same time or slightly later does not contain megacrysts but resembles the granitic metatexite in geochemical composition except for its lower K and REE contents. Later, at around 1840–1815 Ma, a partial melting event occurred in the area, and resulted in leucogranites that have high K-contents and rather low Rb/Sr ratios.

Unlike the mainly granodioritic early Svecofennian granitoids elsewhere in the southern Finland Subprovince, the granitic metatexites contain high amounts of potassium and LREE. The late Svecofennian migmatization event was also different in the study area, being water-fluxed rather than driven by dehydration melting.

Indications of fluid activity in the area is found from different stages of the orogeny. During the early orogeny, excess potassium concentrated in quartz-feldspar paragneisses in the area, possibly from fluids that were co-magmatic to the protolith of the granitic metatexite. During the late Svecofennian, aqueous fluids initiated partial melting in the area. Also, some time during the late Svecofennian, an altered leucogranite was depleted in silica and enriched in potassium by fluids.

Acknowledgements

We are grateful to reviewers Dr. Åke Johansson and Dr. Raimo Lahtinen and editor Dr. Jarmo Kohonen for their help in improving the manuscript. We thank Martin Whitehouse, Kerstin Lindén and Lev Ilyinsky at the NordSIMS facility for the geochronological analysis; NordSIMS was supported by Swedish Research Council infrastructure grant 2014-06375 at the time of these analyses; this is publication # 775). We also thank Tvärminne Zoological Station for granting us access to the study area. We are grateful to Pietari Skyttä for drone images. Grants from Nordenskiöld-samfundet i Finland, Svenska kulturfonden, Victoriastiftelsen, and the Graduate school at Åbo Akademi University made this work possible. Fieldwork was supported by the K. H. Renlund foundation and Forströmsstiftelsen and the SIMS analysis costs were covered by Åbo Akademis Jubileumsfond 1968.

Supplementary data

Electronic Appendices are available via Bulletin of the Geological Society Finland web page.

Electronic Appendix A: U-Pb ion microprobe data and calibration summary.

Electronic Appendix B: Complete whole rock geochemical data set and analytical methods.

References

Andersen, T. & Rämö, O.T. 2021. Dehydration Melting and Proterozoic Granite Petrogenesis in a Collisional Orogen—A Case from the Svecofennian of Southern Finland. Journal of Earth Science, https://doi.org/10.1007/s12583-020-1385-8

Bonin, B., Janoušek, V. & Moyen, J.F. 2020. Chemical variation, modal composition and classification of granitoids. Geological Society Special Publication, 491, 9–51, https://doi.org/10.1144/SP491-2019-138

Boynton, W.V. 1984. Chapter 3 - Cosmochemistry of the Rare Earth Elements: Meteorite Studies. In: Henderson, P. B. T.-D. in G. (ed.) Rare Earth Element Geochemistry.

63–114., https://doi.org/10.1016/B978-0-444-42148-7.50008-3

Bredenberg, E. 2019. Tonalit migmatit i södra Finland – åldersbestämning och petrografisk analys. MSc Thesis, Åbo Akademi University, Finland. 48p.

Brown, M. 1994. The generation, segregation, ascent and emplacement of granite magma: the migmatite-to-crustally-derived granite connection in thickened orogens. Earth Science Reviews, 36, 83–130, https://doi.org/10.1016/0012-8252(94)90009-4

Brown, M. 2013. Granite: From genesis to emplacement. Bulletin of the Geological Society of America, 125, 1079–1113, https://doi.org/10.1130/B30877.1

Bucholz, C.E. & Ague, J.J. 2010. Fluid flow and Al transport during quartz-kyanite vein formation, Unst, Shetland Islands, Scotland. Journal of Metamorphic Geology, 28, 19–39, https://doi.org/10.1111/j.1525-1314.2009.00851.x

Chappell, B.W. & White, A.J.R. 1974. Two contrasting granite types. Pacific Geology, 8, 173–174.

Chopin, F., Korja, A., Nikkilä, K., Hölttä, P., Abdel Zaher, M., Kurhila, M., Eklund, O. & Rämö, O.T. 2020. The Vaasa Migmatitic Complex (Svecofennian Orogen, Finland): Buildup of a LP-HT Dome During Nuna Assembly. Tectonics, 39, https://doi.org/10.1029/2019TC005583

De Saint Blanquat, M., Horsman, E., Habert, G., Morgan, S., Vanderhaeghe, O., Law, R. & Tikoff, B. 2011. Multiscale magmatic cyclicity, duration of pluton construction, and the paradoxical relationship between tectonism and plutonism in continental arcs. Tectonophysics, 500, 20–33, https://doi.org/10.1016/j.tecto.2009.12.009

Dipple, G.M. & Ferry, J.M. 1992. Metasomatism and fluid flow in ductile fault zones. Contributions to Mineralogy and Petrology, 112, 149–164, https://doi.org/10.1007/BF00310451

Edelman, N. 1954. Nötö. Geological Map of Finland 1:100 000, pre-Quaternary rocks, sheet 1033, Geological Survey of Finland.

Edelman, N. 1960. The Gullkrona region, SW Finland. Bulletin de la Commission Géologique de Finlande, 187, 1–87.

Edelman, N. & Jaanus-Järkkälä, M. 1983. A Plate tectonic interpretation of the Precambrian of the Archipelago of southwestern Finland. Geological Survey of Finland, Bulletin, 325, 33.

Ehlers, C., Lindroos, A. & Selonen, O. 1993. The late Svecofennian granite-migmatite zone of southern Finland-a belt of transpressive deformation and granite emplacement. Precambrian Research, 64, 295–309, https://doi.org/10.1016/0301-9268(93)90083-E

Elliott, B.A. 2003. Petrogenesis of the Post-kinematic Magmatism of the Central Finland Granitoid Complex II; Sources and Magmatic Evolution. Journal of Petrology, 44, 1681–1701, https://doi.org/10.1093/petrology/egg053

EMODnet Bathymetry Consortium. 2018. EMODnet Digital Bathymetry (DTM 2018). http://doi.org/10.12770/18ff0d48-b203-4a65-94a9-5fd8b0ec35f6

Frost, B.R. & Frost, C.D. 2008. A Geochemical Classification for Feldspathic Igneous Rocks. Journal of Petrology, 49, 1955–1969, https://doi.org/10.1093/petrology/egn054

Frost, B.R., Barnes, C.G., Collins, W.J., Arculus, R.J., Ellis, D.J. & Frost, C.D. 2001. A geochemical classification for granitic rocks. Journal of Petrology, 42, 2033–2048, https://doi.org/10.1093/petrology/42.11.2033

Frost, C.D., Frost, B.R. & Beard, J.S. 2016. On silica-rich granitoids and their eruptive equivalents. American Mineralogist, 101, 1268–1284, https://doi.org/10.2138/am-2016-5307

García-Arias, M., Corretgé, L.G., Fernández, C. & Castro, A. 2015. Water-present melting in the middle crust: The case of the Ollo de Sapo gneiss in the Iberian Massif (Spain). Chemical Geology, 419, 176–191, https://doi.org/10.1016/j.chemgeo.2015.10.040

Geological Survey of Finland. 2001. Geological Map of the Fennoscandian Shield, Finnish Section. GTK basic licence 1.1, imported from Hakku service on 10 May 2022. https://tupa.gtk.fi/paikkatieto/meta/geological_map_of_the_fennoscandian_shield_1m_finnish_section.html

Geological Survey of Finland. 2018. Rock Geochemical Data of Finland. GTK open licence CC BY 4.0, imported from Hakku service on 30 August 2021. https://tupa.gtk.fi/paikkatieto/meta/rock_geochemical_data_of_finland.html

Geological Survey of Finland. 2014. Bedrock of Finland 1:200 000, 2.3. GTK open licence CC BY 4.0, imported from Hakku service on 12 January 2021. https://tupa.gtk.fi/paikkatieto/meta/bedrock_of_finland_200k.html

Hermansson, T., Stephens, M.B., Corfu, F., Page, L.M. & Andersson, J. 2008. Migratory tectonic switching, western Svecofennian orogen, central Sweden: Constraints from U/Pb zircon and titanite geochronology. Precambrian Research, 161, 250–278, https://doi.org/10.1016/j.precamres.2007.08.008

Hopgood, A.M. 1984. Structural evolution of Svecokarelian migmatites, southern Finland: A study of Proterozoic crustal development. Transactions of the Royal Society of Edinburgh: Earth Sciences, 74, 229–264.

Hopgood, A.M., Bowes, D.R. & Addison, J. 1976. Structural development of migmatites near Skåldö, southwest Finland. Bulletin of the Geological Society of Finland, 48, 43–62, https://doi.org/10.17741/bgsf/48.1-2.005.

Hopgood, A.M., Bowes, D.R., Kouvo, O. & Halliday, A.N. 1983. U-Pb and Rb-Sr isotopic study of polyphase deformed migmatites in the Svecokarelides, Southern Finland. In: Atherton, M. P. and Gribble, C. D. (eds) Migmatites, Melting and Metamorphism. 80–92.

Huhma, H. 1986. Sm-Nd, U-Pb and Pb-Pb isotopic evidence for the origin of the Early Proterozoic Svecokarelian crust in Finland. Geological Survey of Finland, Bulletin, 337, 1–48.

Hölttä, P. & Heilimo, E. 2017. Metamorphic map of Finland. Geological Survey of Finland, Special Paper, 60, 9–40.

Inger, S. & Harris, N. 1993. Geochemical Constraints on Leucogranite Magmatism in the Langtang Valley, Nepal Himalaya. Journal of Petrology, 34, 345–368, https://doi.org/10.1093/petrology/34.2.345

Janoušek, V., Farrow, C.M. & Erban, V. 2006. Interpretation of Whole-rock Geochemical Data in Igneous Geochemistry: Introducing Geochemical Data Toolkit (GCDkit). Journal of Petrology, 47, 1255–1259, https://doi.org/10.1093/petrology/egl013

Jarrard, R.D. 2003. Subduction fluxes of water, carbon dioxide, chlorine, and potassium. Geochemistry, Geophysics, Geosystems, 4, 2002GC000392, https://doi.org/10.1029/2002GC000392

Jeon, H. & Whitehouse, M.J. 2015. A Critical Evaluation of U–Pb Calibration Schemes Used in SIMS Zircon Geochronology. Geostandards and Geoanalytical Research, 39, 443–452, https://doi.org/10.1111/j.1751-908X.2014.00325.x

Johannes, W., Ehlers, C., Kriegsman, L.M. & Mengel, K. 2003. The link between migmatites and S-type granites in the Turku area, southern Finland. Lithos, 68, 69–90, https://doi.org/10.1016/S0024-4937(03)00032-X

Johnson, B.R. & Glazner, A.F. 2010. Formation of K-feldspar megacrysts in granodioritic plutons by thermal cycling and late-stage textural coarsening. Contributions to Mineralogy and Petrology, 159, 599–619, https://doi.org/10.1007/s00410-009-0444-z

Kara, J., Väisänen, M., Johansson, Å., Lahaye, Y., O'Brien, H. & Eklund, O. 2018. 1.90-1.88Ga arc magmatism of central fennoscandia: Geochemistry, U-Pb geochronology, Sm-Nd and Lu-Hf isotope systematics of plutonic-volcanic rocks from southern Finland. Geologica Acta, 16, 1–23, https://doi.org/10.1344/GeologicaActa2018.16.1.1

Kara, J., Väisänen, M., Heinonen, J.S., Lahaye, Y., O'Brien, H. & Huhma, H. 2020. Tracing arclogites in the Paleoproterozoic Era – A shift from 1.88 Ga calc-alkaline to 1.86 Ga high-Nb and adakite-like magmatism in central Fennoscandian Shield. Lithos, 372–373, 105663, https://doi.org/10.1016/j.lithos.2020.105663

Kirkland, C.L., Smithies, R.H., Taylor, R.J.M., Evans, N. & McDonald, B. 2015. Zircon Th/U ratios in magmatic environs. Lithos, 212–215, 397–414, https://doi.org/10.1016/j.lithos.2014.11.021

Korja, A., Lahtinen, R. & Nironen, M. 2006. The Svecofennian orogen: A collage of microcontinents and island arcs. Geological Society Memoir, 32, 561–578, https://doi.org/10.1144/GSL.MEM.2006.032.01.34

Kurhila, M. 2011. Late Svecofennian Leucogranites of Southern Finland : Chronicles of an Orogenic Collapse. PhD Thesis, University of Helsinki, Finland, 23p.

Kurhila, M., Vaasjoki, M., Mänttäri, I., Rämö, O.T. & Nironen, M. 2005. U-Pb ages and Nd isotope characteristics of the lateorogenic, migmatizing microcline granites in southwestern Finland. Bulletin of the Geological Society of Finland, 77, 105–128, https://doi.org/10.17741/bgsf/77.2.002

Kurhila, M., Andersen, T. & Rämö, O.T. 2010. Diverse sources of crustal granitic magma: Lu-Hf isotope data on zircon in three Paleoproterozoic leucogranites of southern Finland. Lithos, 115, 263–271, https://doi.org/10.1016/j.lithos.2009.12.009

Kurhila, M., Mänttäri, I., Vaasjoki, M., Tapani Rämö, O. & Nironen, M. 2011. U–Pb geochronological constraints of the late Svecofennian leucogranites of southern Finland. Precambrian Research, 190, 1–24, https://doi.org/10.1016/j.precamres.2011.07.008

Kähkönen, Y. 2005. Svecofennian supracrustal rocks. In: Lehtinen, M., Nurmi, P. A. & Rämö, O. T. B. T.-D. in P. G. (eds) Precambrian Geology of Finland Key to the Evolution of the Fennoscandian Shield. 343–405., https://doi.org/10.1016/S0166-2635(05)80009-X

Lahtinen, R. 1996. Geochemistry of palaeoproterozoic supracrustal and plutonic rocks in the Tampere-Hämeenlinna area, southern Finland: with 5 tables. Geological Survey of Finland, Bulletin, 389, 113.

Lahtinen, R., Korja, A. & Nironen, M. 2005. Paleoproterozoic Tectonic Evolution. In: Lehtinen, M., Nurmi, P. A. and Rämo, O. T. (eds) Precambrian Geology of Finland- Key to the Evolution of the Fennoscandian Shield. 481–532., https://doi.org/10.1016/S0166-2635(05)80012-X

Lahtinen, R., Korja, A., Nironen, M. & Heikkinen, P. 2009. Palaeoproterozoic Accretionary Processes in Fennoscandia. Cawood, P. A. and Kröner, A. (eds), https://doi.org/10.1144/SP318.8

Lahtinen, R., Salminen, P.E., Sayab, M., Huhma, H., Kurhila, M. & Johnston, S.T. 2022. Age and structural constraints on the tectonic evolution of the Paleoproterozoic Saimaa orocline in Fennoscandia. Precambrian Research, 369, 106477, https://doi.org/10.1016/j.precamres.2021.106477

Laitala, M. 1970. Hanko. Geological Map of Finland 1:100 000, pre-Quaternary rocks, sheet 2011, Geological Survey of Finland.

Laitala, M. 1973. Jussarö. Geological Map of Finland 1:100 000, pre-Quaternary rocks, sheet 2013, Geological Survey of Finland.

Luukas, J., Kousa, J., Nironen, M. & Vuollo, J. 2017. Major stratigraphic units in the bedrock of Finland, and an approach to tectonostratigraphic division. Geological Survey of Finland, Special Paper, 60, 9–40.

Massonne, H.-J. 1992. Evidence for low-temperature ultrapotassic siliceous fluids in subduction zone environments from experiments in the system K2O-MgO-Al2O3-SiO2-H2O (KMASH). Potassic and ultrapotassic magmas and their origin, 28, 421–434, https://doi.org/10.1016/0024-4937(92)90017-S

Mengel, K., Richter, M. & Johannes, W. 2001. Leucosome-forming small-scale geochemical processes in the metapelitic migmatites of the Turku area Finland.

Lithos, 56, 47–73, https://doi.org/10.1016/S0024-4937(00)00059-1

Middlemost, E.A.K. 1994. Naming materials in the magma/igneous rock system. Earth-Science Reviews, 37, 215–224, https://doi.org/10.1016/0012-8252(94)90029-9

Mouri, H., Väisänen, M., Huhma, H. & Korsman, K. 2005. Sm-Nd garnet and U-Pb monazite dating of high-grade metamorphism and crustal melting in the West Uusimaa area, southern Finland. GFF, 127, 123–128, https://doi.org/10.1080/11035890501272123

Mäkitie, H., O'Brien, H., Selonen, O. & Kurhila, M. 2019. The 1.79 Ga Särkilahti leucogranite – a horizontal magma layer below granulite-grade migmatites in SE Finland. Bulletin of the Geological Society of Finland, 91, 179–198, https://doi.org/10.17741/bgsf/91.2.003

Nabelek, P.I. 2020. Petrogenesis of leucogranites in collisional orogens. Geological Society, London, Special Publications, 491, 179 LP – 207, https://doi.org/10.1144/SP491-2018-181

Nevalainen, J., Väisänen, M., Lahaye, Y., Heilimo, E. & Fröjdö, S. 2014. Svecofennian intra-orogenic gabbroic magmatism: A case study from turku, southwestern finland. Bulletin of the Geological Society of Finland, 86, 93–112, https://doi.org/10.17741/bgsf/86.2.003

Nikkilä, K., Mänttäri, I., Nironen, M., Eklund, O. & Korja, A. 2016. Three stages to form a large batholith after terrane accretion – An example from the Svecofennian orogen. Precambrian Research, 281, 618–638, https://doi.org/10.1016/j.precamres.2016.06.018

Nironen, M. 2003. Keski-Suomen granitoidikompleksi. Karttaselitys. Summary: Central Finland Granitoid Complex – Explanation to a map. Tutkimusraportti 157 – Report of Investigation 157.

Nironen, M. 2011. The Pyhäntaka formation, Southern Finland: A sequence of metasandstones and metavolcanic rocks upon an intra-orogenic unconformity. Bulletin of the Geological Society of Finland, 83, 5–23, https://doi.org/10.17741/bgsf/83.1.001

Nironen, M. & Kurhila, M. 2008. The Veikkola granite area in southern Finland: Emplacement of a 1.83–1.82 Ga plutonic sequence in an extensional regime. Bulletin of the Geological Society of Finland, 80, 39–68, https://doi.org/10.17741/bgsf/80.1.003

Nironen, M., Kousa, J., Luukas, J. and Lahtinen, R. 2016. Geological Map of Finland - Bedrock 1 : 1 000 000.

Nironen, M., Luukas, J., Kousa, J., Vuollo, J., Hölttä, P. & Heilimo, E. 2017. Bedrock of Finland at the Scale 1:1 000 000 – Major Stratigraphic Units, Metamorphism and Tectonic Evolution. Nironen, M. (ed.).

Nordbäck, N., Ovaskainen, N., Markovaara-Koivisto, M., Skyttä, P., Ojala, A., Engström, J. & Nixon, C. 2023. Multiscale mapping and scaling analysis of the censored brittle structural framework within the crystalline bedrock of southern Finland. Bulletin of the Geological Society of Finland, 95, 5–32, https://doi.org/10.17741/bgsf/95.1.001

Nurmi, P.A. & Haapala, I. 1986. The Proterozoic granitoids of Finland: granite types, metallogeny and relation to crustal evolution. Bulletin of the Geological Society of Finland, 58, 203–233, https://doi.org/10.17741/bgsf/58.1.014

O'Connor, J.T. 1965. A classification for quartz-rich igneous rocks based on feldspar ratios. US Geological Survey Professional Paper, B525, 79–84.

Patchett, J. & Kouvo, O. 1986. Origin of continental crust of 1.9-1.7 Ga age: Nd isotopes and U-Pb zircon ages in the Svecokarelian terrain of South Finland. Contributions to Mineralogy and Petrology, 92, 1–12, https://doi.org/10.1007/BF00373959

Patiño Douce, A.E. 1999. What do experiments tell us about the relative contributions of crust and mantle to the origin of granitic magmas? Geological Society, London, Special Publications, 168, 55 LP – 75, https://doi.org/10.1144/GSL.SP.1999.168.01.05

Pearce, J. 1996. Sources and settings of granitic rocks. Episodes, 19, 120–125.

Peccerillo, A. & Taylor, S.R. 1976. Geochemistry of eocene calc-alkaline volcanic rocks from the Kastamonu area, Northern Turkey. Contributions to Mineralogy and Petrology, 58, 63–81, https://doi.org/10.1007/BF00384745

Saalmann, K., Mänttäri, I., Ruffet, G. & Whitehouse, M.J. 2009. Age and tectonic framework of structurally controlled Palaeoproterozoic gold mineralization in the Häme belt of southern Finland. Precambrian Research, 174, 53–77, https://doi.org/10.1016/j.precamres.2009.06.005

Salminen, P. & Kurhila, M. 2024. New age constraints for metasedimentary rocks in southern Finland. Bulletin of the Geological Society of Finland, 95, 83–106, https://doi.org/10.17741/bgsf/95.2.001

Sawyer, E.W. 2008. Working with Migmatites: Nomenclature for the Constituent Parts. In: Sawyer, E. W. and Brown, M. (eds) Working with Migmatites. 1–28., https://doi.org/10.2138/gselements.15.5.340

Sawyer, E.W. 2010. Migmatites formed by water-fluxed partial melting of a leucogranodiorite protolith: Microstructures in the residual rocks and source of the fluid. Lithos, 116, 273–286, https://doi.org/10.1016/j.lithos.2009.07.003

Schreurs, J. & Westra, L. 1986. The thermotectonic evolution of a Proterozoic, low pressure, granulite dome, West Uusimaa, SW Finland. Contributions to Mineralogy and Petrology, 93, 236–250, https://doi.org/10.1007/BF00371326

Schwindinger, M., Weinberg, R.F. & Clos, F. 2019. Wet or dry? The difficulty of identifying the presence of water during crustal melting. Journal of Metamorphic Geology, 37, 339–358, https://doi.org/10.1111/jmg.12465

Sederholm, J.J. 1907. Om granit och gneis: deras uppkomst, uppträdande och utbredning inom urberget i Fennoskandia. Bulletin de la Commission Géologique de Finlande, 23, 110.

Sederholm, J.J. 1926. On migmatites and associated Pre-Cambrian rocks of southwestern Finland – Part II: The region around the Barösundsfjärd W. of Helsingfors and neighbouring areas. Bulletin de la Commission Géologique de Finlande, 77.

Selonen, O., Ehlers, C. & Lindroos, A. 1996. Structural features and emplacement of the late Svecofennian Perniö granite sheet in southern Finland. Bulletin of the Geological Society of Finland, 68, 5–17, https://doi.org/10.17741/bgsf/68.2.001

Skyttä, P. 2007. Svecofennian Crustal Evolution in the Uusimaa Belt Area, SW Finland. PhD Thesis, Geological Survey of Finland, Espoo. 17 p.

Stephens, M.B. 2020. Outboard-migrating accretionary orogeny at 1.9–1.8 Ga (Svecokarelian) along a margin to the continent Fennoscandia. Geological Society, London, Memoirs, 50, 237 LP – 250, https://doi.org/10.1144/M50-2019-18

Stephens, M.B. & Andersson, J. 2015. Migmatization related to mafic underplating and intra- or back-arc spreading above a subduction boundary in a 2.0-1.8Ga accretionary orogen, Sweden. Precambrian Research, 264, 235–257, https://doi.org/10.1016/j.precamres.2015.04.019

Stephens, M.B. & Jansson, N.F. 2020. Chapter 6 Paleoproterozoic (1.9–1.8 Ga) syn-orogenic magmatism, sedimentation and mineralization in the Bergslagen lithotectonic unit, Svecokarelian orogen. Geological Society, London, Memoirs, 50, 155 LP – 206, https://doi.org/10.1144/M50-2017-40

Stålfors, T. & Ehlers, C. 2006. Emplacement mechanisms of late-orogenic granites: Structural and geochemical evidence from southern Finland. International Journal of Earth Sciences, 95, 557–568, https://doi.org/10.1007/s00531-005-0049-3

Suikkanen, E., Huhma, H., Kurhila, M. & Lahaye, Y. 2014. The age and origin of the Vaasa migmatite complex revisited. Bulletin of the Geological Society of Finland, 86, 41–55, https://doi.org/10.17741/bgsf/86.1.003

Suominen, V. 1991. The chronostratigraphy of southwestern Finland with special reference to Postjotnian and Subjotnian diabases. Geological Survey of Finland, Bulletin, 356, 100

Torvela, T. & Kurhila, M. 2022. Timing of syn-orogenic, high-grade transtensional shear zone formation in the West Uusimaa Complex, Finland. Bulletin of the Geological Society of Finland, 94, 5–22, https://doi.org/10.17741/bgsf/94.1.001

Vehkamäki, T. 2019. A Multidisciplinary Investigation of the Barösund Shear Zone Area, Southern Finland. MSc Thesis, University of Turku, Finland, 65 p.

Vernon, R.H. & Paterson, S.R. 2002. Igneous origin of K-feldspar megacrysts in deformed granite of the Papoose Flat Pluton, California, USA. Visual Geosciences, 7, 1–28, https://doi.org/10.1007/s10069-002-0005-3

Villaseca, C., Barbero, L. & Herreros, V.V. 1998. A re-examination of the typology of peraluminous granite types in intracontinental orogenic belts. Transactions of the Royal Society of Edinburgh: Earth Sciences, 89, 113–119, https://doi.org/10.1017/S0263593300007045

Väisänen, M. & Hölttä, P. 1999. Structural and metamorphic evolution of the Turku migmatite complex, southwestern Finland. Bulletin of the Geological Society of Finland, 71, 177–218, https://doi.org/10.17741/bgsf/71.1.009

Väisänen, M. & Mänttäri, I. 2002. 1.90–1.88 Ga arc and back-arc basin in the Orijärvi area, SW Finland. Bulletin of the Geological Society of Finland, 74, 185–214.

Väisänen, M., Eklund, O., Lahaye, Y., O'Brien, H., Fröjdö, S., Högdahl, K. & Lammi, M. 2012a. Intra-orogenic Svecofennian magmatism in SW Finland constrained by LA-MC-ICP-MS zircon dating and geochemistry. Gff, 134, 99–114, https://doi.org/10.1080/11035897.2012.680606

Väisänen, M., Johansson, Å., Andersson, U.B., Eklund, O. & Hölttä, P. 2012b. Palaeoproterozoic adakite-and TTG-like magmatism in the Svecofennian orogen, SW Finland. Geologica Acta, 10, 351–371, https://doi.org/10.1344/105.000001761

Weinberg, R.F. & Hasalová, P. 2015. Water-fluxed melting of the continental crust: A review. Lithos, 212–215, 158–188, https://doi.org/10.1016/j.lithos.2014.08.021

Whitehouse, M.J. & Kamber, B.S. 2005. Assigning dates to thin gneissic veins in high-grade metamorphic terranes: A cautionary tale from Akilia, southwest Greenland. Journal of Petrology, 46, 291–318, https://doi.org/10.1093/petrology/egh075

Wiedenbeck, M., Allé, P., Corfu, F., Griffin, W.L., Meier, M., Oberli, F., Von Quadt, A., Roddick, J.C. & Spiegel, W. 1995. Three Natural Zircon Standards for U-Th-Pb, Lu-Hf, Trace Element and REE Analyses. Geostandards Newsletter, 19, 1–23, https://doi.org/10.1111/j.1751-908X.1995.tb00147.x

Wolfram, L.C., Weinberg, R.F., Nebel, O., Hamza, K., Hasalová, P., Míková, J. & Becchio, R. 2019. A 60-Myr record of continental back-arc differentiation through cyclic melting. Nature Geoscience, 12, 215–219, https://doi.org/10.1038/s41561-019-0298-6